Neuroscience 261 (2014) 23–42

INVOLVEMENT OF CANNABINOID RECEPTORS IN PERIPHERAL AND SPINAL MORPHINE ANALGESIA

J. DESROCHES, [a] **J.-F. BOUCHARD,** [b] **L. GENDRON** [c,d,e*] **AND P. BEAULIEU** [a,f*]

[a] *Department of Pharmacology, Université de Montréal, Montréal, Québec, Canada*

[b] *Faculty of Medicine and School of Optometry, Université de Montréal, Montréal, Québec, Canada*

[c] *Department of Physiology and Biophysics, Faculty of Medicine and Health Sciences, Université de Sherbrooke, Sherbrooke, Québec, Canada*

[d] *Centre de recherche clinique Etienne-Le bel, Université de Sherbrooke, Sherbrooke, Québec, Canada*

[e] *Institut de pharmacologie de Sherbrooke, Université de Sherbrooke, Sherbrooke, Québec, Canada*

[f] *Department of Anesthesiology, Université de Montréal, Montréal, Québec, Canada*

Abstract—The interactions between the cannabinoid and opioid systems for pain modulation are reciprocal. However, the role and the importance of the cannabinoid system in the antinociceptive effects of opioids remain uncertain. We studied these interactions with the goal of highlighting the involvement of the cannabinoid system in morphine-induced analgesia. In both phases of the formalin test, intra paw and intrathecal morphine produced similar antinociceptive effects in C57BL/6, cannabinoid type 1 and type 2 receptor wild-type (respectively *cnr1*WT and *cnr2*WT) mice. In *cnr1* and *cnr2* knockout (KO) mice, at the dose used the antinociceptive effect of intra paw morphine in the inflammatory phase of the formalin test was decreased by 87% and 76%, respectively. Similarly, the antinociceptive effect of 0.1 µg spinal morphine in the inflammatory phase was abolished in *cnr1*KO mice and decreased by 90% in *cnr2*KO mice. Interestingly, the antinociceptive effect of morphine in the acute phase of the formalin test was only reduced in *cnr1*KO mice. Notably, systemic morphine administration produced similar analgesia in all genotypes, in both the formalin and the hot water immersion tail-flick tests. Because the pattern of expression of the mu opioid receptor (MOP), its binding properties and its G protein coupling remained unchanged across genotypes, it is unlikely that the loss of morphine analgesia in the *cnr1*KO and *cnr2*KO mice is the consequence of MOP malfunction or downregulation due to the absence of its heterodimerization with either the CB_1 or the CB_2 receptors, at least at the level of the spinal cord.

Key words: cannabinoid receptors, mu opioid receptors (MOP), morphine, pain, tail-flick test, formalin test.

INTRODUCTION

Among several pharmacological properties, analgesia is the most common feature shared by the cannabinoid and opioid systems (Manzanares et al., 1999; Massi et al., 2001). The cannabinoid and opioid receptors display similar properties. They both belong to the $G_{i/o}$ protein-coupled receptor family and are coupled to similar intracellular signaling mechanisms (Bidaut-Russell et al., 1990; Childers et al., 1992; Howlett, 1995). Indeed, the cannabinoids mediate their pharmacological effects through at least two types of receptors, namely CB_1 (Matsuda et al., 1990) and CB_2 (Munro et al., 1993). The anatomical distribution of the CB_1 receptor is consequent with its functions, including the modulation of pain perception at the central, spinal and peripheral levels (Hohmann, 2002; Walczak et al., 2005, 2006; Agarwal et al., 2007; Lever and Rice, 2007). By contrast, CB_2 receptor expression seems to be found predominantly in the peripheral tissues (Munro et al., 1993; Galiegue et al., 1995; Schatz et al., 1997; Jhaveri et al., 2007). However, the expression of this receptor has also been described on brainstem neurons (Van Sickle et al., 2005) and in microglial cell cultures (Beltramo et al., 2006). Opioids mediate their pharmacological effects mainly through three types of receptors: mu (MOP) (Yasuda et al., 1993), delta (DOP) (Evans et al., 1992; Kieffer et al., 1992) and kappa (KOP) (Chen et al., 1993). Although they are found throughout the central nervous system (CNS) and in the peripheral tissues, opioid receptors are primarily expressed at high levels in several brain areas involved in pain perception (Pol and Puig, 2004; Bodnar, 2012).

*Corresponding authors. Address: Department of Physiology and Biophysics, Faculty of Medicine and Health Sciences, Université de Sherbrooke, Sherbrooke, Québec, Canada. Tel: +1-819-820-6868x12760; fax: +1-819-820-6887 (L. Gendron). Address: Department of Pharmacology, Université de Montréal, Montréal, Québec, Canada. Tel: +1-514-343-6338; fax: +1-514-343-2291 (P. Beaulieu).
E-mail addresses: Louis.Gendron@USherbrooke.ca (L. Gendron), pierre.beaulieu@umontreal.ca (P. Beaulieu).

Abbreviations: 2-AG, 2-arachidonoylglycerol; ANOVA, analysis of variance; A.U.C., area under the curve; CNS, central nervous system; cpm, counts per minute; DOP, delta opioid receptor; EDTA, ethylenediaminetetraacetic acid; HEPES, 2-[4-(2-hydroxyethyl)piperazin-1-yl]ethanesulfonic acid; KO, knockout; MOP, mu opioid receptor; MPE, Maximal Possible Effect; PFA, paraformaldehyde; PB, phosphate buffer; PBS, phosphate-buffered saline.

0306-4522 © 2013 The Authors. Published by Elsevier Ltd. Open access under CC BY-NC-ND license.
http://dx.doi.org/10.1016/j.neuroscience.2013.12.030

Interactions between the two systems for pain modulation are reciprocal. Although the role of opioids in cannabinoid antinociceptive effects has been documented (Maldonado and Valverde, 2003; Cichewicz, 2004), there is little information regarding the involvement of the cannabinoid system in the antinociceptive mechanisms of opioids. Indeed, it was recently demonstrated that the CB_1 antagonist AM251 counteracts morphine-induced antinociception in an inflammatory pain model (da Fonseca Pacheco et al., 2008; Pacheco Dda et al., 2009) and in the tail-flick test in mice (Pacheco Dda et al., 2009). These observations led to the hypothesis that MOP activation could induce local release of endocannabinoids and that the subsequent peripheral (da Fonseca Pacheco et al., 2008) or central (Pacheco Dda et al., 2009) activation of the cannabinoid receptors CB_1 and/or CB_2 could contribute to the antinociceptive effects of morphine. A role for the endocannabinoid system in the inhibition of MOP mRNA expression and signaling was also recently described (Paldyova et al., 2008), demonstrating that intraperitoneal administration of the CB_2 antagonist SR144528 attenuates MOP activity through CB_2 cannabinoid receptors (Paldy et al., 2008; Paldyova et al., 2008).

While experiments using pharmacological tools to modify cannabinoid signaling suggested that endocannabinoids are clearly involved in the antinociceptive effects of opioids, studies using transgenic mice are not conclusive. Thus, the role and the importance of the cannabinoid system in the antinociceptive effects of opioids remain uncertain. The aim of this study was therefore to investigate whether opioid and cannabinoid systems can interact at various levels of the neuraxis. We evaluated the role of the cannabinoid system in peripheral (i.e. local injection), spinal and systemic antinociception induced by the activation of MOP following morphine administration in C57BL/6, *cnr1*WT, *cnr1*KO, *cnr2*WT and *cnr2*KO mice.

EXPERIMENTAL PROCEDURES

Animals

Male C57BL/6, *cnr1*WT, *cnr1*KO, *cnr2*WT and *cnr2*KO mice (25–30 g at the time of testing) were used in the current study. They were housed in groups of two to four in standard plastic cages with sawdust bedding in a climate-controlled room. The mice were maintained under a 14-h light/dark cycle (light period 06:00–20:00 h). All experiments were conducted between 07:00 and 12:00 h. The mice were allowed free access to food pellets and water. The C57BL/6 mice were purchased from Charles River, St-Constant, Quebec, Canada, whereas the *cnr1* and *cnr2* transgenic mice were obtained from Pr. Beat Lutz (Institute of Physiological Chemistry and Pathobiochemistry, University of Mainz, Germany) and Jackson Laboratory (Bar Harbor, ME, USA), respectively. These colonies were maintained in-house. This research protocol was approved by the Local Animal Care Committees at the Université de Montréal and Université de Sherbrooke and all procedures conformed to the directives of the Canadian Council on Animal Care and guidelines of the International Association for the Study of Pain. All animal experiments were designed to minimize the number of animals used and their suffering.

Drugs

Morphine sulfate (Morphine HP® 50, lot #151034; Sandoz, Boucherville, QC, Canada) was diluted in a sterile saline solution (0.9% NaCl). Drugs were administered into the dorsal surface of the left hind paw (i.paw), intrathecally (i.t.) or subcutaneously (s.c.) before intradermal (i.d.) formalin injection into the plantar surface of the left hind paw. Morphine was administered i.paw (1 μg/10 μL), i.t. (0.1 μg/5 μL), and s.c. (3 mg/kg for the formalin test or 1, 3 and 10 mg/kg for the tail-flick test). Intrathecal injections were performed in non-anesthetized mice as described previously (Fairbanks, 2003; Gendron et al., 2007). Briefly, a 30-G ½ needle mounted on a 10-μL Luer-tip Hamilton syringe (VWR) was inserted into the L5–L6 intervertebral space, and 5 μL of morphine was injected. Saline was used as vehicle control. The appropriate placement of the needle was confirmed by the observation of a light flick of the tail.

Behavioral studies

Formalin test. The formalin test is a well-established model of tonic pain that is characterized by a transient, biphasic nociceptive response (Tjolsen et al., 1992). The first phase is characterized by the acute activation of sensory receptors. The second phase involves an inflammatory reaction in the peripheral tissue and the development of CNS sensitization. The mice were acclimatized to the testing environment (a clear Plexiglas box 30 × 30 × 30 cm) for 15–20 min or until the cessation of explorative behavior. Thereafter, drugs were injected i.paw, i.t., or s.c. with saline or morphine 5 or 10 min before a 10-μL i.d. injection of a 2% formaldehyde solution (i.e., 5.4% formalin, Fisher Scientific, Montreal, QC, Canada) into the plantar surface of the left hind paw. The experimenter was blind to the drug treatments during testing. Following each injection, the mice were immediately placed in the observation chamber. Nociceptive behaviors were observed for 60 min with the help of a mirror angled at 45° below the observation chamber to allow for an unobstructed view of the hind paws.

The nocifensive behaviors were assessed using a weighted score, as described previously (Dubuisson and Dennis, 1977; Coderre et al., 1993). Following an injection of formalin into the left hind paw, the nociceptive mean score was determined for each 3-min block during the 60-min recording period. In each 3-min bin, the total time the animal spent in four different behavioral categories was recorded: (0), the injected paw is comparable to the contralateral paw and is used normally by the animal; (1), the injected paw has little or no weight placed on it; (2), the injected paw is elevated and is not in contact with any surface; and (3), the

injected paw is licked, bitten or shaken. The weighted nociceptive score ranged from 0 to 3 and was calculated by multiplying the time (in seconds) spent in each category by its assigned category weight, summing these products and dividing by the total time for each 3-min block of time. Nociceptive behavior was thus rated using the following formula: Pain score = (1T1 + 2T2 + 3T3)/180.

The area under the curve (A.U.C.) of "pain score-time" above the weighted pain score of 1 was calculated for the acute phase (0–9 min; Phase I) and the inflammatory phase (21–60 min; Phase II) by the trapezoidal rule using Prism 5.01.

Hot-water immersion tail-flick test. To test the antinociceptive effects of s.c. morphine, tail-flick latencies were measured in C57BL/6, *cnr1*WT, *cnr1*KO, *cnr2*WT and *cnr2*KO mice. The experimenter was blind to the genotype during all testing. Briefly, two centimeters of the tail was immersed in a water bath apparatus (IITC Life Science Inc., Woodland Hills, CA, USA) maintained at 52 ± 0.5 °C. Latency to response was determined by a vigorous tail flick. Baseline measurements were obtained for each mouse before s.c. morphine injection (zero time) and determined from the average of three consecutive trials on the day of the experiment. Subsequently, s.c. injection of morphine (1, 3 and 10 mg/kg) was carried out, and latencies to tail withdrawal were measured every 10 min for a 60-min period. A cut-off time of 10 s was imposed to minimize tissue damage. If an animal reached the cut-off, the tail was removed from the water, and the animal was assigned the maximum score. The percentage of the Maximal Possible Effect (MPE) of s.c. morphine was calculated according to the formula: %MPE = 100 × [(test latency) − (baseline latency)]/[(cut-off time) − (baseline latency)].

Peripheral hind paw edema

At the end of the formalin test, maximal paw thickness was measured at the base of the ipsilateral left hind paw (i.e., formalin-injected hind paw) using a digital micrometer (Mitutoyo Corporation, Aurora, IL, USA) with a resolution of 1 μm (Petricevic et al., 1978; Guindon et al., 2007). The level of inflammation induced by formalin injection in all genotypes was also evaluated by measuring the volume of the hind paw with a plethysmometer (IITC Life Science Inc., Woodland Hills, CA, USA). The hind paw was placed in a small water bath and the volume displacement was measured. Two measurements were carried out for both the ipsi- and the contralateral hind paw, 60 min after formalin injection. Data are expressed as the percentage (%) of paw volume relative to the total body weight of the animal.

Saturation binding assays

Saturation binding assays using mouse spinal cord were performed to determine the affinity (K_d) and the number (B_{max}) of spinal MOP binding sites for each genotype (n = 3 independent experiments per genotype). First, naive mice were briefly anesthetized with isoflurane 5% and euthanized. The spinal cord was then rapidly dissected by laminectomy and pooled (n = 5 spinal cords per assay) in tubes containing 15 mL of ice-cold 50 mM Tris buffer at pH 7.4 with protease inhibitors (buffer A) until homogenization. Afterward, freshly isolated mouse spinal cords were homogenized using a Polytron PT-10-35 (Kinematica, Inc., Bohemia, NY, USA) at 20,000 rpm on ice for 40 s. The homogenates were centrifuged at 15,000 rpm (JA 25.50 rotor; Beckman Coulter) for 15 min, the supernatant was discarded, and the pellets were then stored at −80 °C until they were used. On the day of the experiment, the pellets were thawed on ice, re-suspended in 15 mL of Tris buffer and centrifuged at 15,000 rpm for 15 min. The supernatant was discarded, and the pellets obtained were re-suspended in 35 mL of Tris buffer. A last centrifugation was performed at 15,000 rpm for 15 min; the supernatant was discarded, and the pellets obtained were finally suspended in 10 mL of ice-cold 50 mM potassium phosphate buffer at pH 7.2.

Saturation binding assays using [^{3}H] DAMGO (range: 0.02–16 nM) (MOP ligand; PerkinElmer, Woodbridge, ON, Canada) were performed in duplicate on aliquots of membrane homogenate using a membrane concentration of 2 mg protein/mL. Protein concentrations were determined by the Lowry method (Lowry et al., 1951) using reagents from Bio-Rad (Bio-Rad Laboratories, Mississauga, ON, Canada). The saturation binding experiments were performed in potassium phosphate buffer, in 5-mL polypropylene tubes (final volume of 500 μL). Non-specific binding was determined in the presence of 1 μM DAMGO. The tubes were incubated for 90 min at 25 °C. The incubation was terminated by filtration using ice-cold potassium phosphate buffer (3 × 2 mL) on a Whatman GF/C filter (GE Healthcare Life Sciences, Piscataway, NJ, USA). The filters were then placed in vials containing scintillation cocktail. The radioactivity present on the disks was determined by liquid scintillation counting using a Beckman Coulter LS-6500 scintillation counter (Beckman Coulter Canada, Inc., Mississauga, ON, Canada). The counts per minute (cpm) were converted into disintegrations per minute (dpm) using the external standard method, and finally, the B_{max} was converted into fmol/mg, whereas the K_d was expressed in nM.

Immunofluorescence

Immunofluorescence was performed to visualize the expression of MOP in spinal cord of *cnr1*WT, *cnr1*KO, *cnr2*WT and *cnr2*KO mice. First, naive mice were briefly anesthetized with 5% isoflurane and perfusion-fixed with ice-cold 4% paraformaldehyde (PFA; Polysciences, Inc., Warrington, PA, USA) in 0.2 M phosphate buffer (PB, pH 7.4) at 4 °C (500 mL). The spinal cord was then isolated by laminectomy, post-fixed in ice-cold 4% PFA for 2 h and cryoprotected in 30% sucrose in 0.2 M PB for 48 h. The lumbar segment L4–L6 was then snap-frozen in −50 °C isopentane and stored at −80 °C until sectioning. Afterward, transverse sections were cut on a microtome (Leica SM2000R; Toronto, Ontario, Canada)

at a thickness of 30 μm and placed in phosphate-buffered saline (PBS). The floating sections were then incubated in 1% sodium borohydride in PBS for 30 min, rinsed twice with PBS, and incubated for 30 min at room temperature in a blocking solution containing 3% normal goat serum (NGS) and 0.3% Triton X-100 in PBS. The sections were then incubated overnight at 4 °C with the guinea pig anti-MOP primary antibody (cat# GP10106; Neuromics, Minneapolis, MN, USA) diluted 1:1000 in the blocking solution. The floating sections were then washed in PBS and incubated with a goat anti-guinea pig secondary antibody conjugated with Alexa Fluor 488 (Molecular Probes, Invitrogen, Carlsbad, CA, USA) at a concentration of 1:1000 in PBS for 2 h at room temperature.

Images were collected using an epifluorescence microscope (Leica DM4000B; Leica Microsystems, Toronto, Ontario, Canada) to visualize MOP expression in laminae I–II of the dorsal horn of the mouse spinal cord ($n = 3$ animals per genotype). The pictures were taken with a 5× objective.

[^{35}S]GTPγS binding assay

[^{35}S]GTPγS binding assays using mouse spinal cords were performed to determine the potency (EC_{50}) and the efficacy (E_{max}) of spinal MOP binding sites for each of the genotypes. First, naive mice were briefly anesthetized with isoflurane 5% and euthanized. The spinal cords were then rapidly collected and pooled ($n = 4$–6 spinal cords per assay) in tubes containing 3 mL of ice-cold buffer (50 mM HEPES, 100 mM NaCl, 5 mM $MgCl_2$, 1 mM EDTA and protease inhibitors, pH 7.4) until homogenization. The freshly isolated mouse spinal cords were then homogenized using a Wheaton Potter–Elvehjem tissue grinder combined with a Teflon pestle inserted in a Wheaton electric overhead stirrer (Fischer Scientific) at approximately 600 rpm on ice, 3 times 5–6 passages. The homogenates were centrifuged at 13,000 rpm (JA 25.15 rotor; Beckman Coulter) for 20 min, the supernatant was discarded, and the pellets were then stored at −80 °C until use. On the day of the experiment, the pellets were thawed on ice, re-suspended in 3 mL of HEPES buffer and centrifuged at 13,000 rpm for 20 min; subsequently, the supernatant was discarded, and the pellets obtained were suspended in 4 mL of ice-cold Tris–HCl buffer. Protein concentrations were determined by the Lowry method (Lowry et al., 1951) using reagents from Bio-Rad (Bio-Rad Laboratories, Mississauga, ON, Canada). Aliquots of spinal cord membrane homogenates were incubated (20 μg of proteins) in duplicate for 2 h at 30 °C in incubation buffer containing 0.1% bovine serum albumin, 1 mM dithiothreitol (DTT), 10 μM guanosine 5′-diphosphate sodium salt (GDP; Sigma, Oakville, ON, Canada), 0.1 nM guanosine 5′(γ-^{35}S-thio) triphosphate tetralithium salt ([^{35}S]GTPγS, 1250 Ci/mmol, Perkin Elmer, Montreal, QC, Canada) and protease inhibitors in the absence or presence of the MOP agonist morphine (0.01 nM–10 μM), in a total volume of 500 μL. Basal [^{35}S]GTPγS binding was assessed in the absence of morphine. Non-specific binding was measured in the presence of 10 μM unlabeled GTPγS. The reaction was terminated by rapid filtration through a Whatman GF/C filter (GE Healthcare Life Sciences, Piscataway, NJ, USA), followed by two washes with 2 mL of ice-cold assay buffer. The filters were placed in vials containing scintillation cocktail. Bound radioactivity on the filters was determined by liquid scintillation counting using a Beckman Coulter LS-6500 scintillation counter (Beckman Coulter Canada, Inc., Mississauga, ON, Canada). cpm were converted to the percentage of increase of the agonist-stimulated [^{35}S]GTPγS binding over the basal binding. The efficacy (E_{max}) was determined by the maximum increase in [^{35}S]GTPγS binding induced by morphine, whereas the potency (EC_{50}) was obtained from a nonlinear regression analysis (Prism 5.01).

Calculation and statistical analysis

Data are expressed as means ± standard error of the mean (SEM). Calculations were performed with Excel 2007, and graphs and statistical analysis were performed using Prism 5.01 (Graph Pad Software, San Diego, CA, USA). Comparisons of means were performed using either a two-tailed unpaired *t*-test, a one-way analysis of variance (ANOVA) or a two-way ANOVA followed by Bonferroni's multiple-comparison test. The binding data from saturation studies were analyzed using nonlinear regression to determine B_{max} and K_d (Prism 5.01). All binding data were best fit by a one-site model. The morphine-stimulated [^{35}S]GTPγS binding data were fit with a sigmoidal 3-parameter function (Prism 5.01) to determine the EC_{50}. The comparison of differences between basal vs. stimulated [^{35}S]GTPγS binding, as well as differences between EC_{50} within the different genotypes was determined by a one-way ANOVA followed by Bonferroni's multiple-comparison test. The critical level of significance was set at 5% ($P < 0.05$).

RESULTS

Intradermal formalin injection induces a similar biphasic nociceptive profile within all genotypes

In the present study, we observed that for all genotypes, formalin injection produced a similar biphasic nociceptive response (acute and inflammatory phases) that is typical of this tonic pain model (Fig. 1). Indeed, nociceptive responses following i.d. formalin injection were not different within genotypes for both phases of the formalin test (Fig. 1A; $P = 0.8949$, $F_{genotypes} = 0.2738$, two-way ANOVA). These nociceptive effects were also compared by separate analyses of the acute and inflammatory phases. There were no differences in the nociceptive effects of i.d. formalin in the acute phase (Fig. 1B; A.U.C., $F = 2.013$, one-way ANOVA) or the inflammatory phase of the formalin test (Fig. 1C; A.U.C., $F = 0.1949$, one-way ANOVA). These results demonstrate that all genotypes present a similar nociceptive profile following i.d. formalin injection into the hind paw in both phases of the formalin test.

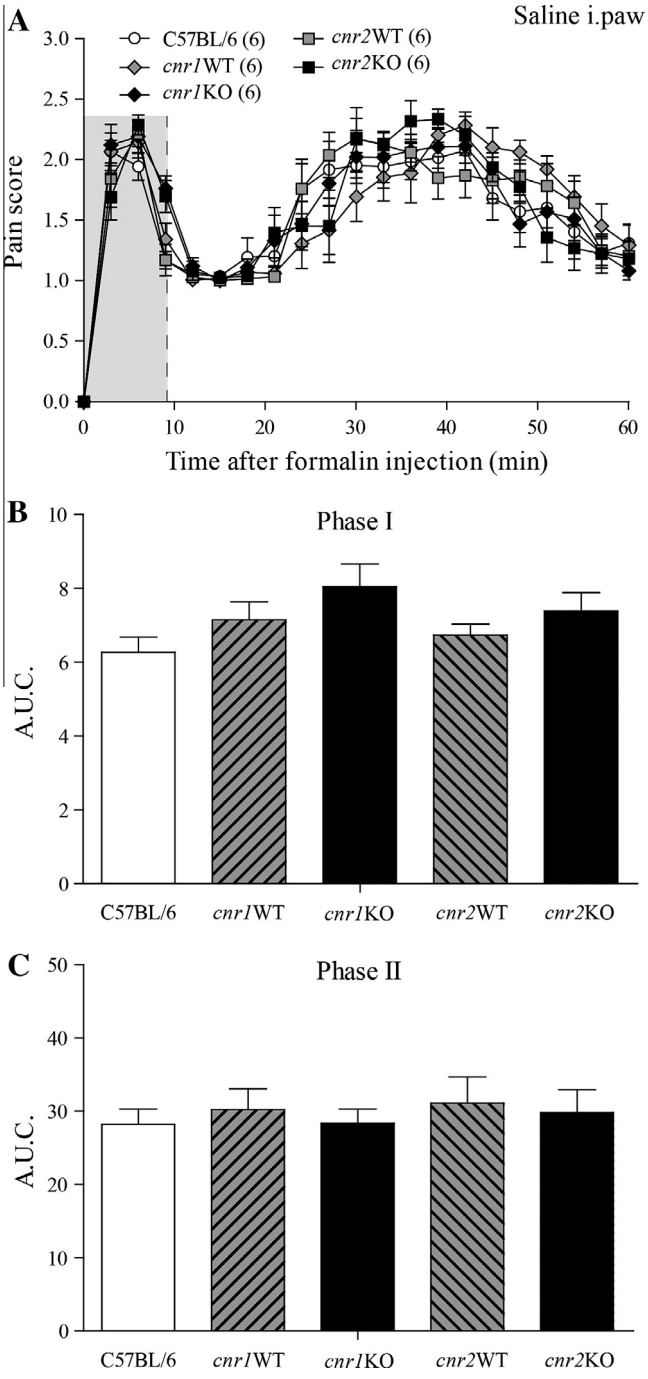

Fig. 1. Nociceptive biphasic profile of intradermal (i.d.) formalin in different genotypes. C57BL/6, *cnr1*WT, *cnr1*KO, *cnr2*WT and *cnr2*KO male mice were injected with 5.4% intradermal formalin (10 μL) in the plantar surface of the left hind paw, and pain behaviors were recorded for 60 min. (A) In the early (0–9 min) (highlighted by a gray area) and late phase (21–60 min) of the formalin test, all genotypes present similar biphasic nociceptive behavioral profiles following formalin injection. (B) The A.U.C. analysis indicates that i.d. formalin injection produces a comparative nociceptive response within all genotypes in the early phase of the formalin test. (C) The A.U.C. analysis of the late phase also reveals that i.d. formalin injection produces a similar nociceptive profile within all genotypes in the late phase. The numbers in parentheses represent the number of animals per group. The data are expressed as means ± SEM.

Involvement of CB_1 cannabinoid receptors in the antinociceptive effects of i.paw morphine in the formalin test

As expected, local (i.paw) morphine (1 μg) induced an inhibition of pain behaviors in the C57BL/6 mice (Fig. 2 vs. Fig. 1). Similarly, i.paw morphine reduced formalin-induced nocifensive behaviors in the *cnr1*WT mice. However, at the same dose, i.paw morphine had no analgesic effects in the *cnr1*KO mice. Thus, compared to the C57BL/6 and *the cnr1*WT mice, the pain scores measured for the *cnr1*KO mice following i.paw morphine injection were significantly higher in both the acute and inflammatory phases of the formalin test (Fig. 2A; $P < 0.0001$, $F_{genotypes} = 81.37$, two-way ANOVA).

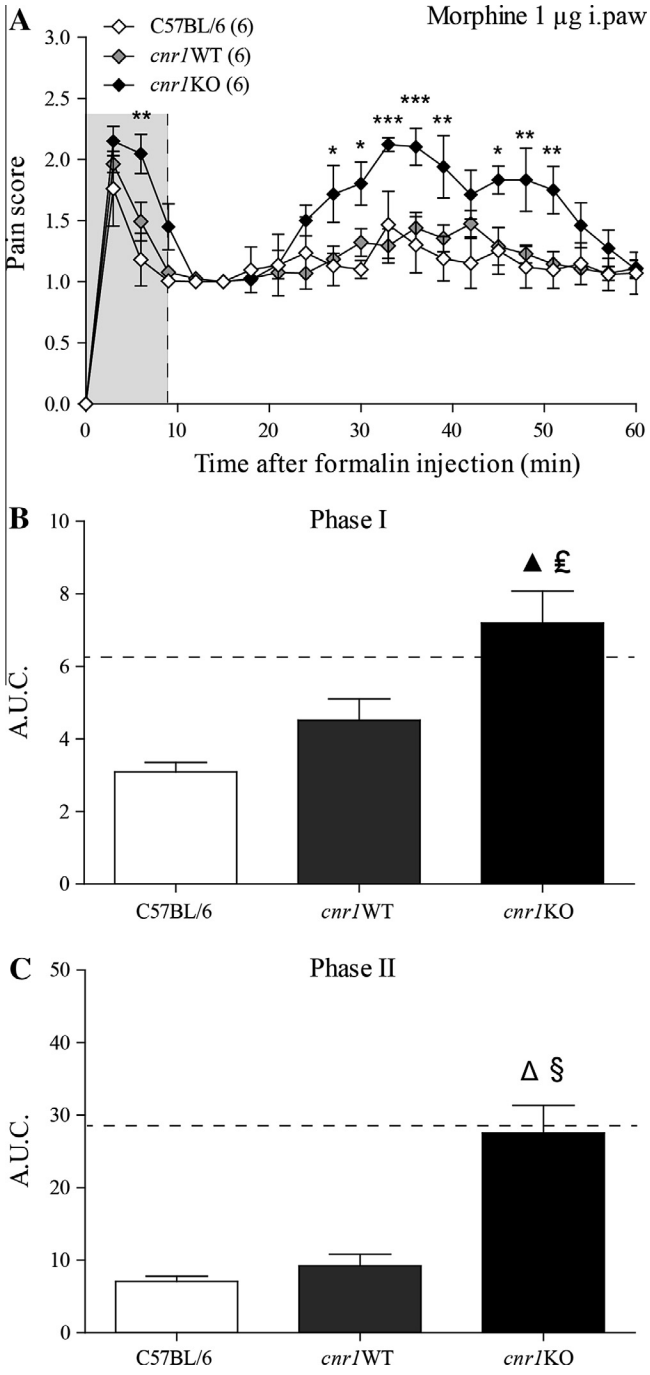

Fig. 2. Loss of antinociceptive effects of i.paw morphine in the *cnr1*KO mice. (A) In the early (highlighted by a gray area) and late phases of the formalin test, the analgesic effects of i.paw morphine (1 µg/10 µL, 5 min prior to formalin injection) are decreased in *cnr1*KO mice compared to *cnr1*WT mice ($^{*}P < 0.05$, $^{**}P < 0.01$, $^{***}P < 0.001$) (two-way ANOVA with Bonferroni's *post hoc* test). (B) The A.U.C. analysis of the early phase reveals a loss of the analgesic effectiveness of i.paw morphine ($^{\blacktriangle}P < 0.001$ for *cnr1*KO vs. C57BL/6 mice; $^{£}P < 0.05$ for *cnr1*KO vs. *cnr1*WT mice). (C) The A.U.C. analysis of the late phase also reveals a loss of the analgesic effectiveness of i.paw morphine ($^{\Delta}P < 0.001$ for *cnr1*KO vs. C57BL/6 mice; $^{§}P < 0.001$ for *cnr1*KO vs. *cnr1*WT mice) (one-way ANOVA with Bonferroni's *post hoc* test). The horizontal dashed lines (panels B and C) represent the A.U.C of the C57BL/6 mice, which received NaCl 0.9% for reference purposes (cf. Fig. 1B, C). The numbers in parentheses represent the number of animals per group. Data are expressed as means ± SEM.

These differences observed in the antinociceptive effects were also confirmed by separate analyses of the acute and inflammatory phases. We observed a significant increase in the A.U.C. for the acute phase (Fig. 2B; A.U.C., 7.2 ± 0.9 for *cnr1*KO vs. 3.1 ± 0.3 for C57BL/6 and 4.5 ± 0.6 for *cnr1*WT; $F = 11.02$, one-way ANOVA) and for the inflammatory phase (Fig. 2C; A.U.C., 27.5 ± 3.8 for *cnr1*KO vs. 7.1 ± 0.8 for C57BL/6 and 9.2 ± 1.6 for *cnr1*WT; $F = 21.54$, one-way ANOVA). These results demonstrate that the i.paw morphine effectiveness is impeded in the *cnr1*KO vs. the *cnr1*WT mice in both phases of the formalin test.

More precisely, under these conditions the analgesic effects of morphine were completely abolished in the acute phase and reduced by 87% in the inflammatory phase (Fig. 2B, C). Such a decrease suggests that CB_1 receptors are important for the complete expression of the analgesic effects of i.paw morphine in both phases of the formalin test.

Involvement of CB_2 cannabinoid receptors in the antinociceptive effects of i.paw morphine in the formalin test

The administration of i.paw morphine (1 μg) induced a decrease in pain behaviors in C57BL/6 mice (Fig. 3 vs. Fig. 1) (for comparative purposes, the results presented for C57BL/6 mice are the same as in Fig. 2). Similarly, i.paw morphine reduced the formalin-induced pain behaviors in the *cnr2*WT mice. However, at the same dose, i.paw morphine lost its antinociceptive properties in the *cnr2*KO mice in the late phase. Indeed, compared to the C57BL/6 and the *cnr2*WT mice, the pain score measured for the *cnr2*KO mice following i.paw morphine injection was significantly higher only in the inflammatory phase of the formalin test (Fig. 3A; $P < 0.0001$, $F_{genotypes} = 40.42$, two-way ANOVA). There were no differences in the antinociceptive effects of i.paw morphine within genotypes when the acute phase of the formalin test was analyzed (Fig. 3B; A.U.C., $F = 1.29$, one-way ANOVA). Conversely, the loss of antinociceptive effects of i.paw morphine in the *cnr2*KO mice over the entire inflammatory phase was confirmed by a significant increase in the A.U.C. compared to the C57BL/6 and the *cnr2*WT mice (Fig. 3C; A.U.C., 26.3 ± 3.9 for *cnr2*KO vs. 7.1 ± 0.8 for C57BL/6 and 11.1 ± 2.8 for *cnr2*WT; $F = 13.23$, one-way ANOVA). Under these conditions, our results demonstrate a loss of i.paw morphine effectiveness of 76% in the *cnr2*KO vs. the *cnr2*WT mice, but only in the inflammatory phase of the formalin test (Fig. 3B, C). Such a decrease suggests that CB_2 receptors are involved in the analgesic effects of i.paw morphine in the inflammatory phase of the formalin test.

Locally mediated antinociceptive effects of i.paw morphine in the formalin test

To confirm that the previously observed antinociceptive effects of i.paw morphine were induced by a local effect of morphine, rather than by a systemic effect, we further injected morphine contralaterally to the formalin injection. In the C57BL/6 mice, i.paw morphine (1 μg) had no analgesic effect when injected in the contralateral hind paw. Thus, pain scores for contralateral i.paw morphine were not different from pain scores measured for animals injected with i.paw saline, but they did differ from pain scores obtained with ipsilateral i.paw morphine injection in both the acute and the inflammatory phases of the formalin test (Fig. 4A; $P < 0.0001$, $F_{treatments} = 98.36$, two-way ANOVA). These differences were also observed when the acute and the inflammatory phases were analyzed separately, as confirmed by the analysis of the acute phase A.U.C. (Fig. 4A, upper inset; A.U.C., 6.7 ± 0.5 for contralateral i.paw morphine vs. 6.3 ± 0.4 for i.paw saline and 3.1 ± 0.3 for i.paw morphine; $F = 25.68$, one-way ANOVA) and the inflammatory phase A.U.C. (Fig. 4A, lower inset; A.U.C., 30.6 ± 1.5 for contralateral i.paw morphine vs. 28.2 ± 2.0 for i.paw saline and 7.1 ± 0.8 for i.paw morphine; $F = 72.09$, one-way ANOVA).

In the *cnr1*WT mice, i.paw morphine (1 μg) had no analgesic effect when injected into the contralateral hind paw. Hence, the pain scores for contralateral i.paw morphine were not different from the pain scores measured for animals injected with i.paw saline, but they did differ from the pain scores obtained with ipsilateral i.paw morphine injection in both the acute and the inflammatory phases of the formalin test (Fig. 4B; $P < 0.0001$, $F_{treatments} = 83.51$, two-way ANOVA). These differences were also observed when the acute and the inflammatory phases were analyzed separately, as confirmed by the analysis of the acute phase A.U.C. (Fig. 4B, upper inset; A.U.C., 6.7 ± 0.3 for contralateral i.paw morphine vs. 7.1 ± 0.5 for i.paw saline and 4.5 ± 0.6 for i.paw morphine; $F = 8.60$, one-way ANOVA) and the inflammatory phase A.U.C. (Fig. 4B, lower inset; A.U.C., 31.4 ± 2.6 for contralateral i.paw morphine vs. 30.2 ± 2.8 for i.paw saline and 9.2 ± 1.6 for i.paw morphine; $F = 26.74$, one-way ANOVA).

In the *cnr2*WT mice, i.paw morphine (1 μg) had no analgesic effect when injected into the contralateral hind paw. Actually, the pain scores for contralateral i.paw morphine were not different from the pain scores measured for animals injected with i.paw saline, but they did differ from the pain scores obtained with ipsilateral i.paw morphine injection in both the acute and the inflammatory phases of the formalin test (Fig. 4C; $P < 0.0001$, $F_{treatments} = 48.85$, two-way ANOVA). These differences were also observed when the acute and the inflammatory phases were analyzed, as confirmed by the analysis of the acute phase A.U.C. (Fig. 4C, upper inset; A.U.C., 6.3 ± 0.4 for contralateral i.paw morphine vs. 6.7 ± 0.3 for i.paw saline and 4.3 ± 0.7 for i.paw morphine; $F = 7.18$, one-way ANOVA) and the inflammatory phase A.U.C. (Fig. 4C, lower inset; A.U.C., 29.5 ± 1.3 for contralateral i.paw morphine vs. 31.1 ± 3.6 for i.paw saline and 11.1 ± 2.8 for i.paw morphine; $F = 16.50$, one-way ANOVA). These observations reveal that the effects of i.paw morphine described in Figs. 2 and 3 are due to its local as opposed to systemic action in the formalin test.

Involvement of CB_1 cannabinoid receptors in the antinociceptive effects of i.t. morphine in the formalin test

Because the analgesic effects of morphine are also mediated by receptors located in the spinal cord, we also studied whether cannabinoid receptors are involved in the effects of i.t. morphine. We observed that i.t. morphine (0.1 μg) induced an inhibition of the nocifensive behaviors in C57BL/6 mice (Fig. 5). Similarly, i.t. morphine reduced the formalin-induced behaviors in the *cnr1*WT mice. However, at the same dose, i.t. morphine had no analgesic effects in the

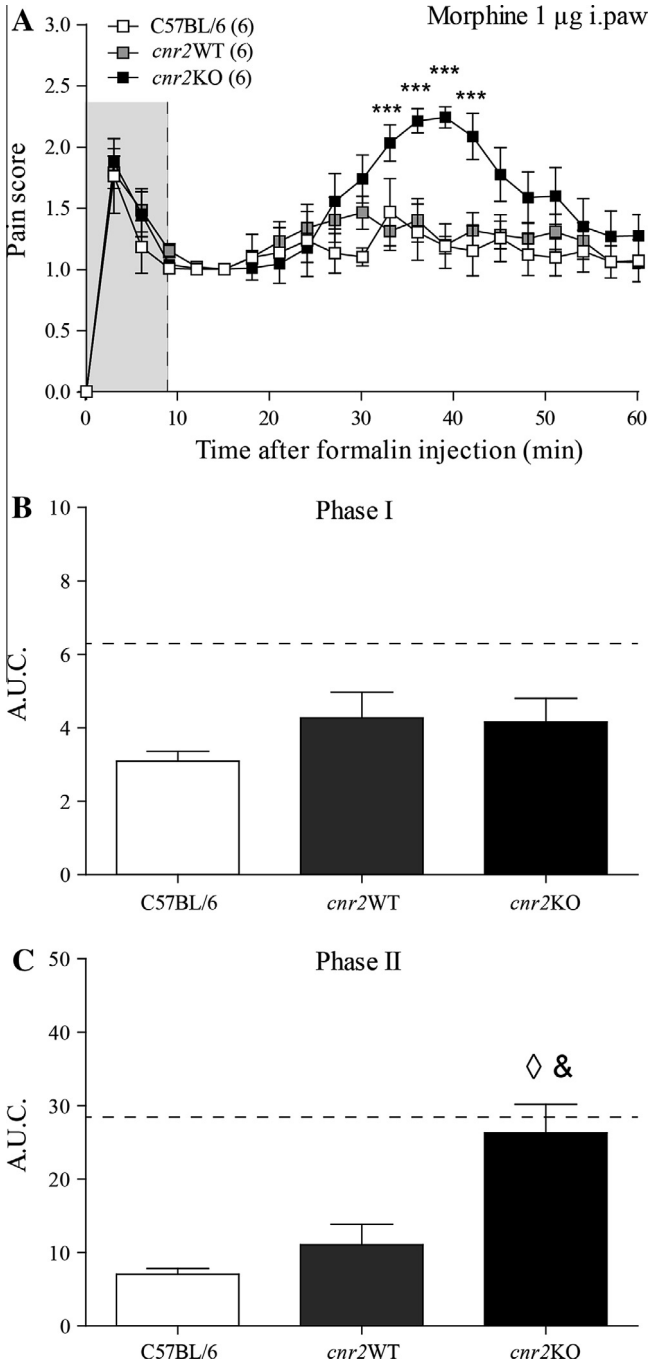

Fig. 3. Loss of antinociceptive effects of i.paw morphine in *cnr2*KO mice. (A) In the late phase of the formalin test, the analgesic effects of i.paw morphine (1 µg/10 µL, 5 min prior to formalin injection) are decreased in *cnr2*KO mice compared to *cnr2*WT mice ($^{***}P < 0.001$) (two-way ANOVA with Bonferroni's *post hoc* test). (B) The A.U.C. analysis reveals that i.paw morphine preserves its analgesic effectiveness in the early phase of the formalin test. (C) The A.U.C. analysis of the late phase reveals a loss of analgesic effectiveness for i.paw morphine ($^{\diamond}P < 0.001$ for *cnr2*KO vs. C57BL/6 mice (for reference purposes, the results presented for the C57BL/6 mice are the same as in Fig. 2); $^{\&}P < 0.01$ for *cnr2*KO vs. *cnr2*WT mice) (one-way ANOVA with Bonferroni's *post hoc* test). The horizontal dashed lines (panels B and C) represent the A.U.C of the C57BL/6 mice, which received NaCl 0.9% for reference purposes (cf. Fig. 1B, C). The numbers in parentheses represent the number of animals per group. Data are expressed as means ± SEM.

*cnr1*KO mice. In fact, compared to the C57BL/6 and *the cnr1*WT mice, the pain score measured for the *cnr1*KO mice following i.t. morphine injection was significantly higher both in the acute and the inflammatory phases of the formalin test (Fig. 5A; $P < 0.0001$, $F_{genotypes} = 186.90$, two-way ANOVA). These differences observed in the antinociceptive effects were also confirmed by separate analyses of the acute and the inflammatory phases. We observed a significant increase in the acute phase A.U.C. (Fig. 5B; A.U.C., 7.5 ± 0.5 for *cnr1*KO vs. 4.7 ± 0.5 for C57BL/6 and 5.1 ± 0.6 for *cnr1*WT; $F = 8.07$, one-way ANOVA) and

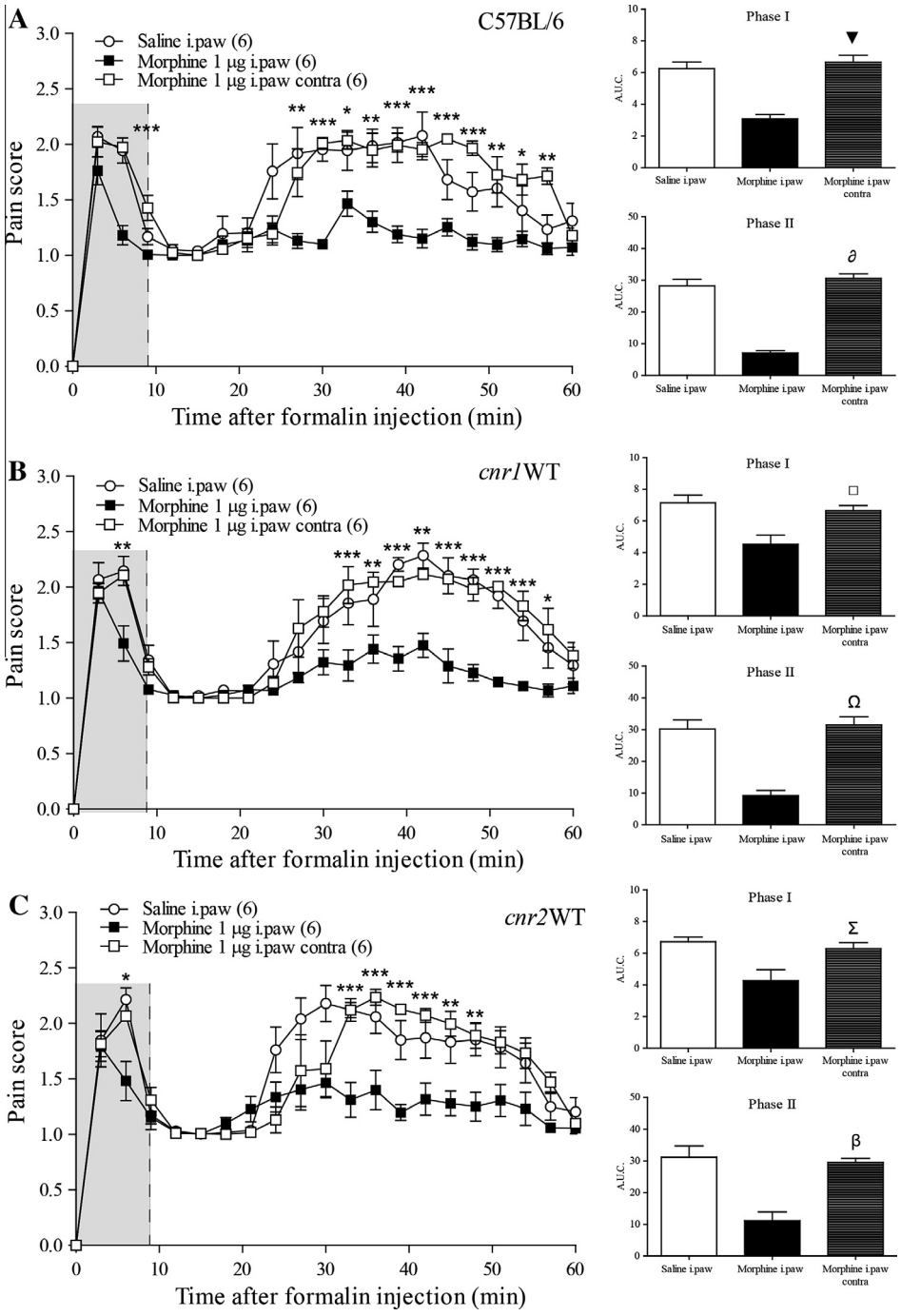

Fig. 4. Contralateral i.paw morphine injection did not inhibit formalin-induced pain behavior. (A) In the early and the late phases of the formalin test in C57BL/6 mice, ipsilateral i.paw morphine (1 μg/10 μL, 5 min prior to formalin injection) produced a decrease in formalin-induced pain behaviors compared to contralateral i.paw morphine ($^{*}P < 0.05$, $^{**}P < 0.01$, $^{***}P < 0.001$) (two-way ANOVA with Bonferroni's *post hoc* test) (for analysis purpose, the results presented for i.paw saline and ipsilateral i.paw morphine were taken from Figs. 1–3). These data show that the antinociceptive effects of i.paw morphine were local rather than systemic. The A.U.C. analyses of the early and late phases of the formalin test validate the absence of antinociceptive effects for contralateral i.paw morphine (Phase I; $^{\blacktriangledown}P < 0.001$ vs. ipsilateral i.paw morphine; Phase II; $^{\partial}P < 0.001$ vs. ipsilateral i.paw morphine) (one-way ANOVA with Bonferroni's *post hoc* test). (B) In the early and late phases of the formalin test in the *cnr1*WT mice, ipsilateral i.paw morphine (1 μg/10 μL, 5 min prior to formalin injection) produced a decrease in the formalin-induced pain behaviors compared to contralateral i.paw morphine ($^{*}P < 0.05$, $^{**}P < 0.01$, $^{***}P < 0.001$) (two-way ANOVA with Bonferroni's *post hoc* test). The A.U.C. analyses of the early and late phases of the formalin test validate the absence of antinociceptive effects for contralateral i.paw morphine (Phase I; $^{\square}P < 0.05$ vs. ipsilateral i.paw morphine; Phase II; $^{\Omega}P < 0.001$ vs. ipsilateral i.paw morphine) (one-way ANOVA with Bonferroni's *post hoc* test). (C) In the early and the late phases of the formalin test in the *cnr2*WT mice, i.paw morphine (1 μg/10 μL, 5 min prior to formalin injection) produced a decrease in formalin-induced pain behaviors compared to contralateral i.paw morphine ($^{*}P < 0.05$, $^{**}P < 0.01$, $^{***}P < 0.001$) (two-way ANOVA with Bonferroni's *post hoc* test). The A.U.C. analyses of the early and late phases of the formalin test validate the absence of antinociceptive effects for contralateral i.paw morphine (Phase I; $^{\Sigma}P < 0.05$ vs. ipsilateral i.paw morphine; Phase II; $^{\beta}P < 0.001$ vs. ipsilateral i.paw morphine) (one-way ANOVA with Bonferroni's *post hoc* test). The numbers in parentheses represent the number of animals per group. Data are expressed as means ± SEM.

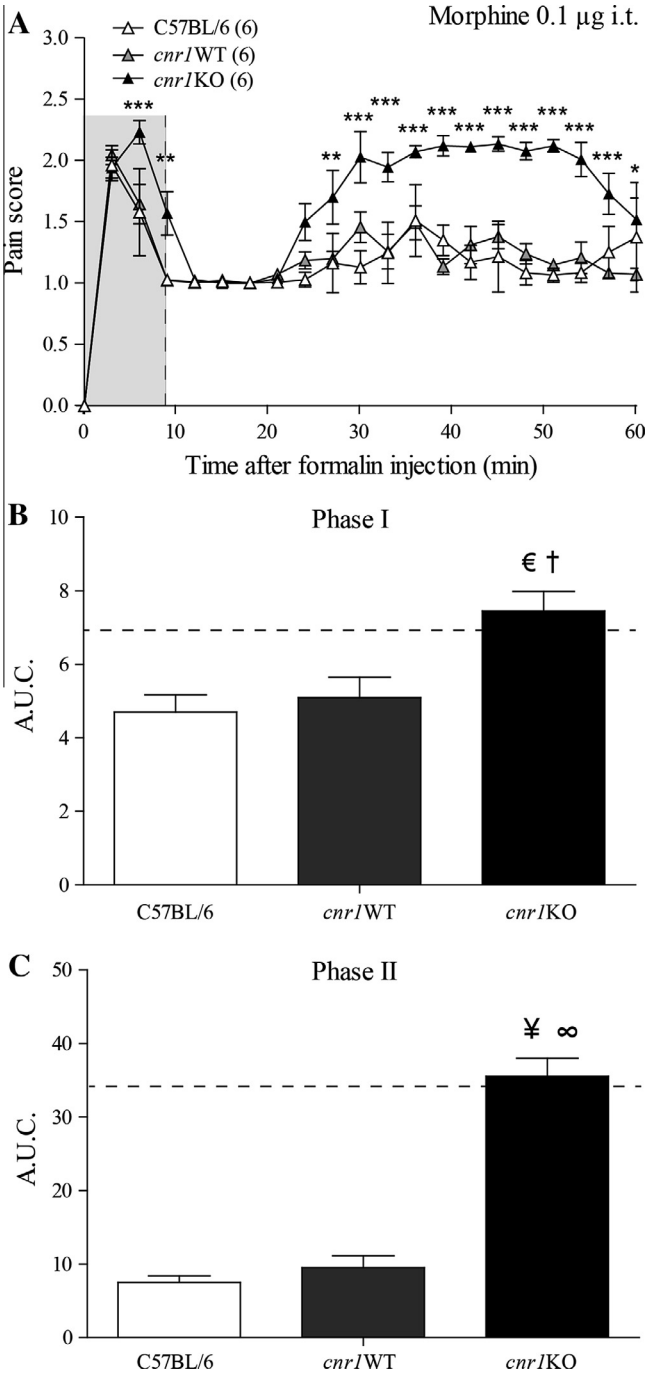

Fig. 5. Loss of antinociceptive effects of i.t. morphine in *cnr1*KO mice. (A) In the early and late phases of the formalin test, the analgesic effects of i.t. morphine (0.1 µg/5 µL, 5 min prior to formalin injection) are decreased in *cnr1*KO mice compared to *cnr1*WT mice ($^{*}P < 0.05$, $^{**}P < 0.01$, $^{***}P < 0.001$) (two-way ANOVA with Bonferroni's *post hoc* test). (B) The A.U.C. analysis of the early phase reveals a loss of the analgesic effectiveness of i.t. morphine ($^{€}P < 0.01$ for *cnr1*KO vs. C57BL/6 mice; $^{†}P < 0.05$ for *cnr1*KO vs. *cnr1*WT mice). (C) The A.U.C. analysis of the late phase also reveals a loss of the analgesic effectiveness of i.t. morphine ($^{¥}P < 0.001$ for *cnr1*KO vs. C57BL/6 mice; $^{∞}P < 0.001$ for *cnr1*KO vs. *cnr1*WT mice) (one-way ANOVA with Bonferroni's *post hoc* test). The numbers in parentheses represent the number of animals per group. Data are expressed as means ± SEM.

the inflammatory phase (Fig. 5C; A.U.C., 35.5 ± 2.5 for *cnr1*KO vs. 7.5 ± 0.9 for C57BL/6 and 9.5 ± 1.6 for *cnr1*WT; $F = 78.42$, one-way ANOVA). These results demonstrate that i.t. morphine analgesia was greatly impaired in the *cnr1*KO mice for both phases of the formalin test. Indeed, at this dose of i.t. morphine, its analgesic effect was almost completely abolished in both phases of the formalin test, thus supporting a major role for CB_1 receptors in the analgesic effects of morphine in this tonic pain context.

Involvement of CB_2 cannabinoid receptors in the antinociceptive effects of i.t. morphine in the formalin test

The injection of i.t. morphine (0.1 μg) induced a robust inhibition of pain behaviors in C57BL/6 mice (Fig. 6) (for comparative purposes, the results presented for C57BL/6 mice are the same as in Fig. 5). Similarly, i.t. morphine reduced the formalin-induced pain behaviors in the *cnr2*WT mice. However, at the same dose, i.t. morphine had no analgesic effects in the *cnr2*KO mice in the late phase. Thus, compared to the C57BL/6 and the *cnr2*WT mice, the pain score measured for the *cnr2*KO mice following i.t. morphine injection was significantly different only in the inflammatory phase of the formalin test (Fig. 6A; $P < 0.0001$,

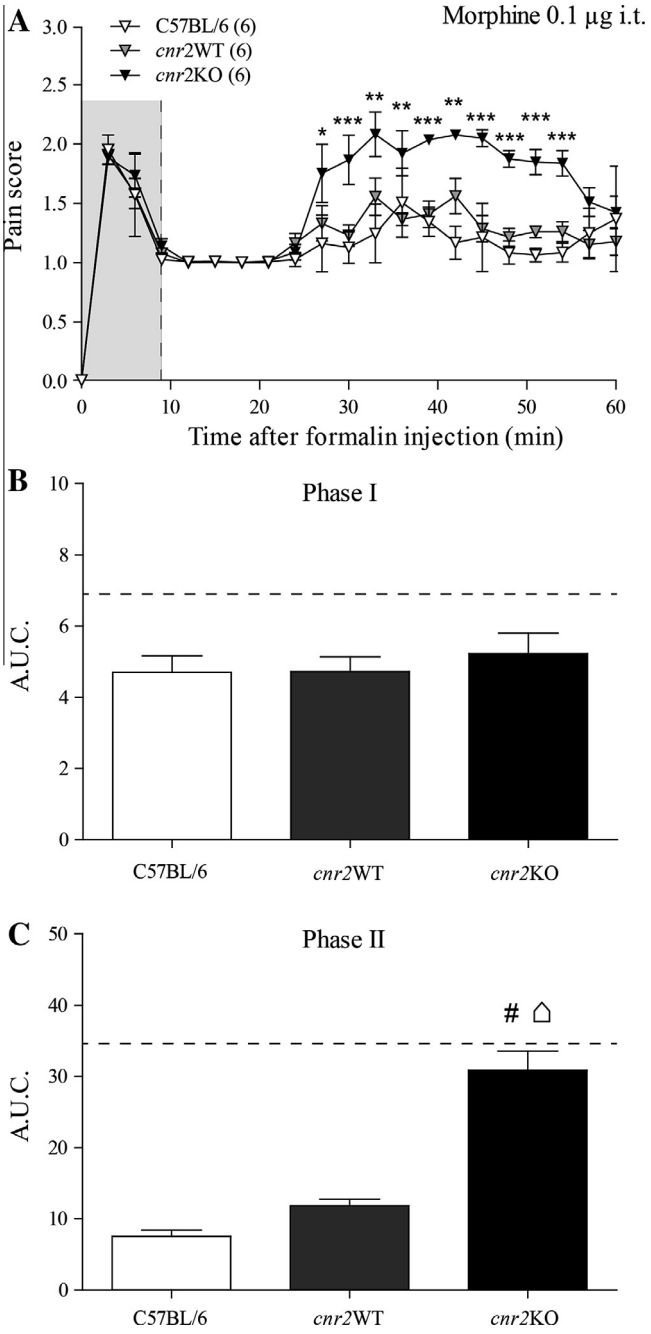

Fig. 6. Loss of antinociceptive effects of i.t. morphine in *cnr2*KO mice. (A) In the late phase of the formalin test, the analgesic effects of i.t. morphine (0.1 μg/5 μL, 5 min prior to formalin injection) are decreased in *cnr2*KO mice compared to *cnr2*WT mice ($^{*}P < 0.05$, $^{**}P < 0.01$, $^{***}P < 0.001$) (two-way ANOVA with Bonferroni's *post hoc* test). (B) The A.U.C. analysis indicates that i.t. morphine preserves its analgesic effectiveness in the early phase of the formalin test. (C) The A.U.C. analysis of the late phase reveals a loss of analgesic effectiveness for i.t. morphine in the late phase ($^{\#}P < 0.001$ for *cnr2*KO vs. C57BL/6 mice (for reference purposes, the results presented for C57BL/6 mice are the same as in Fig. 5); $\triangle P < 0.001$ for *cnr2*KO vs. *cnr2*WT mice) (one-way ANOVA with Bonferroni's *post hoc* test). The numbers in parentheses represent the number of animals per group. Data are expressed as means ± SEM.

$F_{genotypes}$ = 91.94, two-way ANOVA). Indeed, the loss of the antinociceptive effects of i.t. morphine in the *cnr2*KO mice over the entire inflammatory phase was confirmed by a significant increase in the A.U.C. compared to C57BL/6 and *cnr2*WT mice (Fig. 6C; A.U.C., 30.8 ± 2.7 for *cnr2*KO vs. 7.5 ± 0.9 for C57BL/6 and 11.8 ± 0.9 for *cnr2*WT; F = 50.72, one-way ANOVA). The effect of morphine in the acute phase of the formalin test was similar for all genotypes (Fig. 6B; A.U.C., F = 0.37, one-way ANOVA). These results therefore revealed a 90% loss of i.t. morphine effectiveness in the *cnr2*KO vs. the *cnr2*WT mice specifically in the inflammatory phase of the formalin test. Such a decrease suggests that CB_2 receptors have an important role in the analgesic effects of i.t. morphine in the inflammatory phase of the formalin test.

Effect of formalin on thickness and edema of the hind paw

To verify whether the absence of CB_1 or CB_2 receptors impacts the development of formalin-induced inflammation, which in turn might affect the analgesic properties of morphine, we measured the maximal paw thickness and edema following the injection of formalin for various treatments and genotypes.

Both the thickness and the edema (volume) significantly increased in the formalin-injected hind paw vs. the contralateral side 60 min after formalin injection (data not shown). As shown in Table 1, the maximal thickness of the formalin-injected hind paw for each genotype did not differ between treatments (Table 1; P = 0.9036, $F_{treatments}$ = 0.1875 for C57BL/6; P = 0.7126, $F_{treatments}$ = 0.4611 for *cnr1*WT; P = 0.1249, $F_{treatments}$ = 2.157 for *cnr1*KO; P = 0.3699, $F_{treatments}$ = 1.106 for *cnr2*WT; P = 0.1217, $F_{treatments}$ = 2.183 for *cnr2*KO, one-way ANOVA). Similarly, the edema induced by formalin did not differ across treatments within each genotype (Table 1; P = 0.3631, $F_{treatments}$ = 1.124 for C57BL/6; P = 0.2454, $F_{treatments}$ = 1.498 for *cnr1*WT; P = 0.1312, $F_{treatments}$ = 2.108 for *cnr1*KO; P = 0.1443, $F_{treatments}$ = 2.015 for *cnr2*WT; P = 0.0821, $F_{treatments}$ = 2.581 for *cnr2*KO, one-way ANOVA). These results demonstrated that treatments did not influence the maximal thickness or the edema in the formalin test.

Finally, the maximal thickness and the volume of the ipsilateral hind paw were analyzed to observe whether genotype affected the development of inflammation. As shown in Table 1, the maximal thickness of the formalin-injected hind paw did not differ between genotypes (Table 1; P = 0.2765, $F_{genotypes}$ = 1.359 for saline i.paw; P = 0.3497, $F_{genotypes}$ = 1.165 for morphine i.paw; P = 0.9809, $F_{genotypes}$ = 0.1017 for saline i.t.; P = 0.3068, $F_{genotypes}$ = 1.273 for morphine i.t., one-way ANOVA). Moreover, the edema of the formalin-injected hind paw also did not differ between genotypes (Table 1; P = 0.4067, $F_{genotypes}$ = 1.039 for saline i.paw; P = 0.1450, $F_{genotypes}$ = 1.882 for morphine i.paw; P = 0.3496, $F_{genotypes}$ = 1.166 for saline i.t.; P = 0.2178, $F_{genotypes}$ = 1.552 for morphine i.t., one-way ANOVA). These results demonstrated that genotype did not influence the maximal thickness or the edema in the formalin test.

Cannabinoid receptors are not involved in the antinociceptive effects of s.c. morphine in the formalin test

Because a significant contribution of the analgesic effects of morphine is mediated by receptors located in the brain (periaqueductal gray, rostroventral medulla), we also evaluated the contribution of CB_1 and CB_2 receptors following systemic morphine administration. As anticipated, s.c. morphine (3 mg/kg) induced an inhibition of pain behaviors in the C57BL/6 mice, but only in the late phase of the formalin test (Fig. 7). Surprisingly, in contrast to what we observed following

Table 1. Effects of formalin on paw thickness and edema

	Maximal thickness[a] (mm)			
	Saline i.paw	Morphine i.paw	Saline i.t.	Morphine i.t.
C57BL/6	1.96 ± 0.05	1.93 ± 0.08	1.94 ± 0.06	1.90 ± 0.05
*cnr1*WT	1.99 ± 0.02	1.95 ± 0.05	1.93 ± 0.08	2.01 ± 0.05
*cnr1*KO	2.15 ± 0.01	1.95 ± 0.09	1.91 ± 0.05	1.99 ± 0.03
*cnr2*WT	2.04 ± 0.06	2.07 ± 0.05	1.95 ± 0.05	2.00 ± 0.04
*cnr2*KO	2.16 ± 0.12	2.06 ± 0.04	1.96 ± 0.03	1.96 ± 0.03
	Volume[b] (mL/g)%			
	Saline i.paw	Morphine i.paw	Saline i.t.	Morphine i.t.
C57BL/6	0.88 ± 0.03	0.90 ± 0.03	0.85 ± 0.02	0.83 ± 0.04
*cnr1*WT	0.82 ± 0.04	0.87 ± 0.05	0.81 ± 0.06	0.72 ± 0.03
*cnr1*KO	0.83 ± 0.02	0.85 ± 0.04	0.76 ± 0.04	0.76 ± 0.03
*cnr2*WT	0.88 ± 0.03	0.79 ± 0.04	0.77 ± 0.04	0.76 ± 0.05
*cnr2*KO	0.83 ± 0.02	0.79 ± 0.03	0.73 ± 0.04	0.72 ± 0.03

Maximal thickness and edema were evaluated 60 min after formalin injection into the left hind paw.
Data are expressed as means ± SEM (n = 6 per group).
[a] Maximal thickness was measured with a digital micrometer and expressed in mm.
[b] The volume of the inflamed hind paw was determined by water displacement using a plethysmometer and expressed as the percentage of paw volume relative to the total body weight of the animal (mL/g).

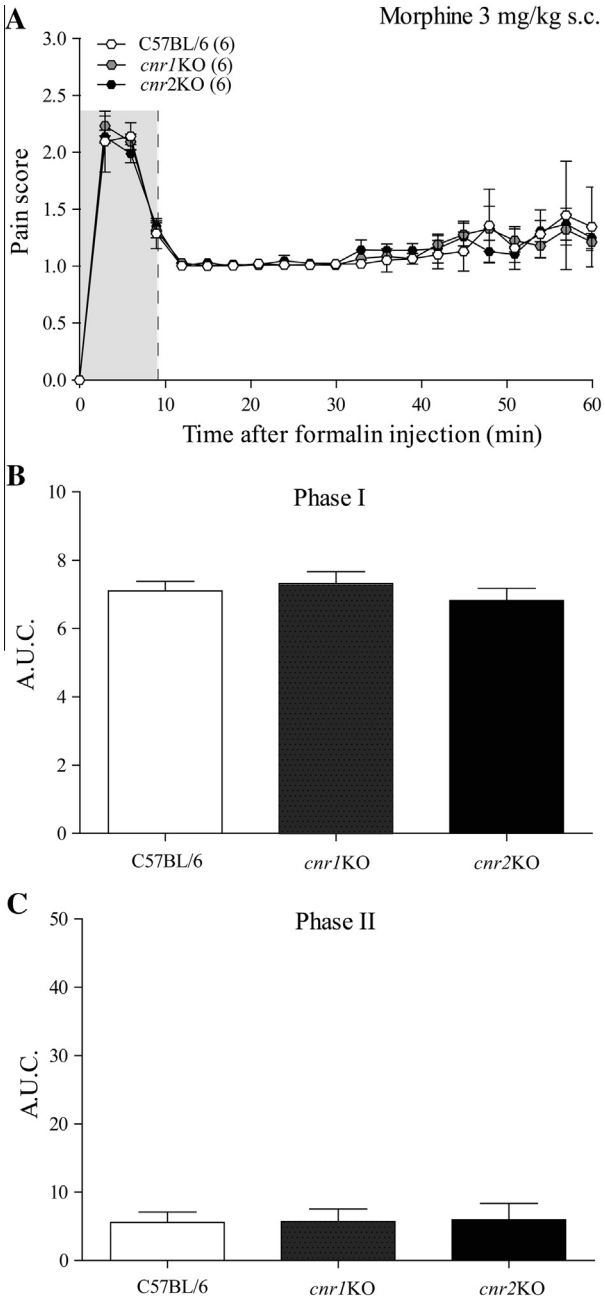

Fig. 7. Antinociceptive effects of s.c. morphine are maintained in the mouse formalin test. All three genotypes (C57BL/6, *cnr1*KO and *cnr2*KO) present similar biphasic nociceptive behavioral profiles following morphine 3 mg/kg s.c. injection (10 min prior to formalin injection). (A) In the late phase of the formalin test, the analgesic effects of s.c. morphine are preserved in *cnr1*KO and *cnr2*KO mice. (B) The A.U.C. analysis indicates that s.c. morphine preserves its analgesic effectiveness in the early phase of the formalin test. (C) The A.U.C. analysis of the late phase also reveals that s.c. morphine preserves its analgesic properties. The numbers in parentheses represent the number of animals per group. Data are expressed as means ± SEM.

i.paw and i.t. morphine (Figs. 2, 3, 5 and 6), s.c. morphine significantly reduced the formalin-induced nocifensive behaviors in the inflammatory phase in the *cnr1*KO and the *cnr2*KO mice (Fig. 7). Hence, pain behaviors following the injection of s.c. morphine were not different within genotypes in both phases of the formalin test (Fig. 7A; $P = 0.9622$, $F_{genotypes} = 0.04$, two-way ANOVA). There were no statistically significant differences in the antinociceptive effects of s.c. morphine when the acute phase of the formalin test was analyzed (Fig. 7B; A.U.C., $F = 0.55$, one-way ANOVA) nor when the inflammatory phase of the formalin test was analyzed (Fig. 7C; A.U.C., $F = 0.01$, one-way ANOVA). Notably, s.c. morphine had no antinociceptive effects in the acute phase: there were no differences in the A.U.C. of s.c. morphine 3 mg/kg compared to saline i.paw (Fig. 7B vs. Fig. 1B; A.U.C., $P = 0.1266$, $t = 1.667$ and df = 10, two-tailed unpaired *t*-test).

Together, our results demonstrate that in contrast to i.paw and i.t. morphine, s.c. morphine preserved its antinociceptive properties in the *cnr1*KO and the *cnr2*KO mice in the inflammatory phase of the formalin test and, therefore, suggest that cannabinoid receptors do not significantly contribute to the analgesic effects of s.c. morphine.

Cannabinoid receptors are not involved in the antinociceptive effects of s.c. morphine in the hot-water immersion tail-flick test

To test whether cannabinoid receptors are involved in the antinociceptive effects of s.c. morphine in acute pain relief, we used the hot-water immersion tail-flick test (tail immersion test in a water bath at 52 °C) to measure the antinociceptive effects of 1, 3 and 10 mg/kg s.c. morphine. As shown in Fig. 8A–C, genotype did not produce any significant difference in the baseline latency to tail withdrawal compared to C57BL/6 mice ($P = 0.1904$, $F_{genotypes} = 1.572$, two-way ANOVA). In all genotypes, s.c. morphine produced a time- and dose-dependent analgesia that peaked at 20 min post-injection ($P < 0.0001$, $F_{time} = 64.57$ for 1 mg/kg s.c. morphine; $P < 0.0001$, $F_{time} = 163.7$ for 3 mg/kg s.c. morphine; $P < 0.0001$, $F_{time} = 583.2$ for 10 mg/kg s.c. morphine, two-way ANOVA). Latency to tail withdrawal returned to baseline by 40 to 60 min after the s.c. morphine injection. The %MPE values of s.c. morphine were calculated from the latencies to tail withdrawal that were obtained 20 min post-injection (Fig. 8D). At any dose, the analgesic effect of s.c. morphine did not differ between genotypes; $\%MPE_{1mg/kg}$ (16.0 ± 2.3% for C57BL/6, 18.3 ± 1.1% for *cnr1*WT, 12.3 ± 2.5% for *cnr1*KO, 19.9 ± 2.4% for *cnr2*WT and 18.3 ± 1.0% for *cnr2*KO; $F = 2.26$), $\%MPE_{3mg/kg}$ (37.7 ± 2.6% for C57BL/6, 37.5 ± 2.3% for *cnr1*WT, 33.6 ± 1.8% for *cnr1*KO, 40.1 ± 2.5% for *cnr2*WT and

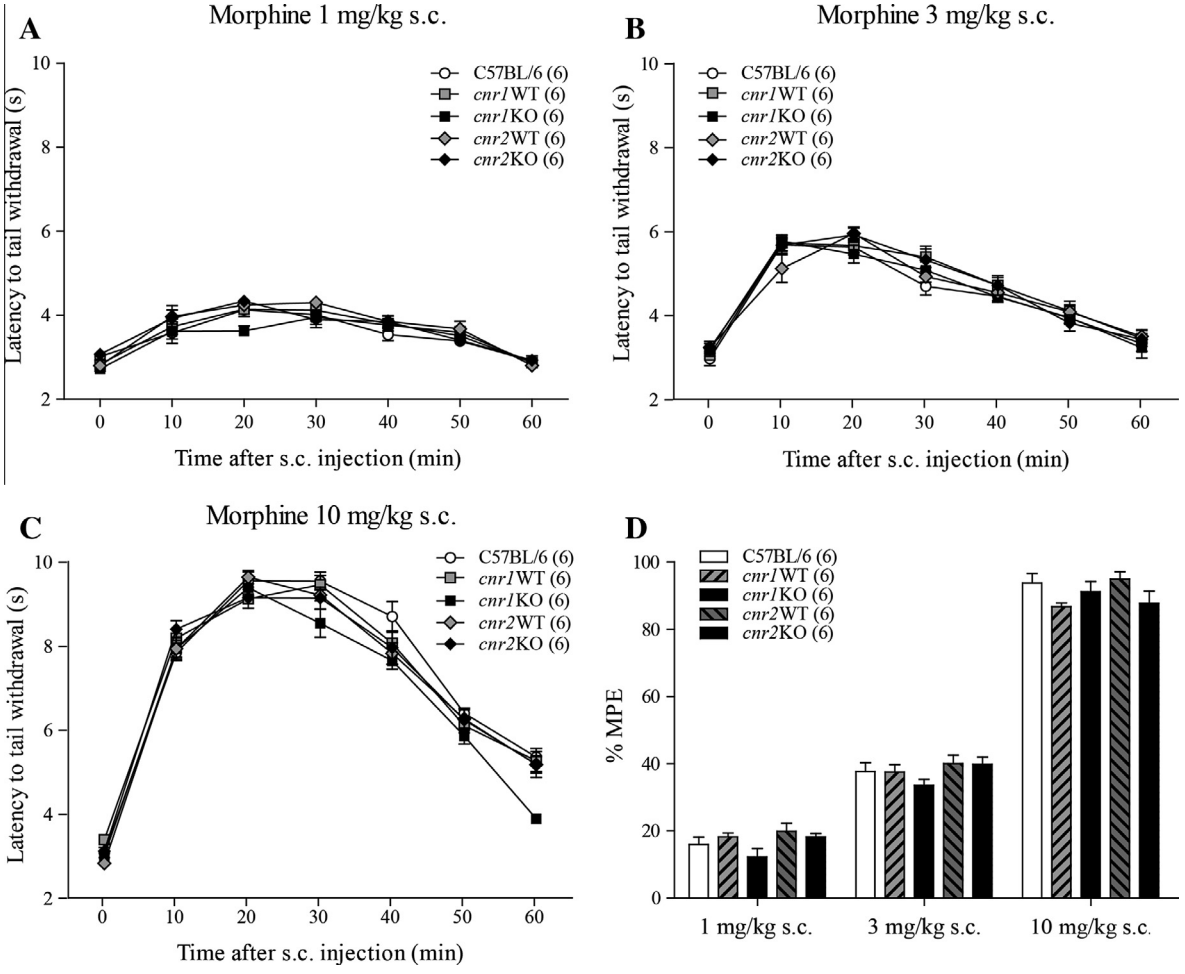

Fig. 8. Antinociceptive effects of s.c. morphine are maintained in the mice tail-flick test. Tail-flick latencies (s) to noxious heat (tail immersion in water at 52 °C) were recorded every 10 min (from 0 to 60 min) following the s.c. injection of morphine 1, 3 and 10 mg/kg in C57BL/6, *cnr1*WT, *cnr1*KO, *cnr2*WT and *cnr2*KO male mice. (A–C) Morphine at 1, 3 and 10 mg/kg produced significant time-dependent antinociception with no difference between genotypes. (D) The %MPE of s.c. morphine at 20 min (peak antinociceptive effects) was calculated for each dose tested. There were no significant differences between genotypes compared to C57BL/6 for each dose tested; thus, genotype did not modify the antinociceptive effects of morphine (one-way ANOVA with Bonferroni's *post hoc* test). The numbers in parentheses represent the number of animals per group. Data are expressed as means ± SEM.

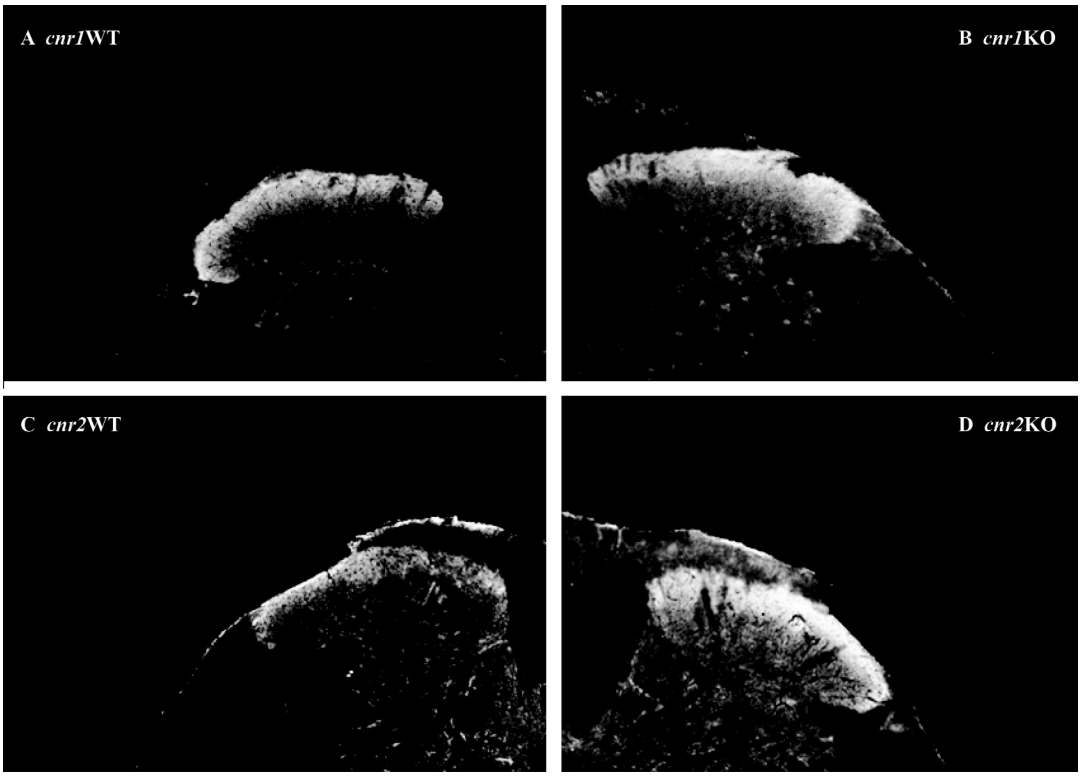

Fig. 9. Deletion of the CB_1 or CB_2 receptors has no effect on the expression of MOP in the spinal cord. Immunofluorescence of spinal MOP revealed that the expression of MOP in laminae I and II of the dorsal horn of the spinal cord did not differ between *cnr1*WT (A) and *cnr1*KO (B) mice or between *cnr2*WT (C) and *cnr2*KO mice (D).

39.9 ± 2.2% for *cnr2*KO; $F = 1.30$) and $\%MPE_{10mg/kg}$ (93.7 ± 2.9% for C57BL/6, 86.7 ± 1.2% for *cnr1*WT, 91.2 ± 3.0% for *cnr1*KO, 95.0 ± 2.2% for *cnr2*WT and 87.8 ± 3.6% for *cnr2*KO; $F = 1.80$, one-way ANOVA).

No differences were detected in spinal MOP expression between the wild-type and the knockout mice using immunofluorescence

In an effort to determine whether the inactivation of CB_1 or CB_2 receptors affects the expression pattern of MOP, we first compared the MOP-like immunofluorescence staining in spinal cords of the *cnr1*WT (Fig. 9A), *cnr1*KO (Fig. 9B), *cnr2*WT (Fig. 9C), and *cnr2*KO mice (Fig. 9D). Although qualitative (at best), the immunofluorescence labeling revealed similar expression patterns of MOP in laminae I and II of the dorsal horn of the spinal cord in all genotypes.

No differences were detected in spinal MOP expression and binding properties between wild-type and knockout mice using saturation binding assays

To verify if the loss of the antinociceptive effects of morphine in the *cnr1*KO and the *cnr2*KO mice could be the consequence of a lower level of MOP expression or of altered binding capacities, we performed saturation binding assays in spinal cord membrane extracts from these mice. As shown in Table 2, [^{3}H]-DAMGO saturation binding assays revealed that the level of spinal MOP (B_{max}) did not significantly differ between the *cnr1*WT and the *cnr1*KO mice ($P = 0.8759$, $t = 0.1664$ and df = 4) or between the *cnr2*WT and the *cnr2*KO mice ($P = 0.8916$, $t = 0.1452$ and df = 4). We further found that the affinity (K_d) of DAMGO for spinal MOP remained unchanged between the *cnr1*WT and the *cnr1*KO mice ($P = 0.5616$, $t = 0.6322$ and df = 4) and between the *cnr2*WT and the *cnr2*KO mice ($P = 0.2424$, $t = 1.370$ and df = 4, two-tailed unpaired *t*-test). Thus, differences observed in i.paw and i.t. morphine analgesic effectiveness are apparently not caused by decreases in the levels of expression or reduced binding affinity of MOP in *cnr1*KO and *cnr2*KO mice, at least at the level of the spinal cord.

Table 2. Binding properties of spinal MOP

	B_{max} [a] (fmol/mg)	K_d [b] (nM)
*cnr1*WT	44.50 ± 2.34	1.75 ± 0.27
*cnr1*KO	43.43 ± 5.99	2.32 ± 0.86
*cnr2*WT	34.32 ± 5.82	2.21 ± 1.03
*cnr2*KO	33.23 ± 4.74	4.70 ± 1.50

[^{3}H]DAMGO saturation binding assays were performed in mouse spinal cord preparations.
Data are expressed as means ± SEM ($n = 3$ per group).
[a] B_{max} represents the amount of MOP binding sites in spinal cord of mice expressed as fmol/mg of protein.
[b] K_d represents the affinity of [^{3}H]DAMGO for MOP in the spinal cord extracts and is expressed in nM.

Table 3. G protein coupling of spinal MOP

	EC_{50}[a] (nM)	E_{max}[b] (Percentage increase over basal binding; %)
C57BL/6	87.50 ± 26.80	29.73 ± 2.93
*cnr1*WT	121.20 ± 38.25	31.86 ± 1.09
*cnr1*KO	105.50 ± 26.93	38.01 ± 3.82
*cnr2*WT	127.60 ± 43.76	37.99 ± 6.97
*cnr2*KO	93.81 ± 15.82	46.83 ± 5.58

[^{35}S]GTPγS binding assays were performed in mouse spinal cord membrane preparations.

Data are expressed as means ± SEM (n = 3 per group).

[a] The potency (EC_{50}) of morphine was determined as the concentration (nM) required to reach 50% of the maximal possible effect (i.e., 50% of the maximal [^{35}S]GTPγS binding).

[b] The efficacy (E_{max}) represents the maximum functional response induced by morphine, i.e., maximal [^{35}S]GTPγS binding, and is expressed as the percentage increase over basal binding (%).

No differences were detected in spinal MOP activity between wild-type and knockout mice using [^{35}S]GTPγS binding assay on mice spinal cord

To assess if the inactivation of CB_1 or CB_2 receptors might alter the G protein coupling of MOP in the spinal cords of transgenic mice, we performed [^{35}S]GTPγS binding assays using spinal cord extracts. As shown in Table 3, the stimulation of [^{35}S]GTPγS binding by morphine was used as a functional measure of the status of G protein coupling to the receptor. We found that morphine increased the binding of [^{35}S]GTPγS in spinal cord extracts with similar potency (EC_{50}) and efficacy (E_{max}) in the C57BL/6 compared to the *cnr1*WT and the *cnr1*KO mice ($P = 0.7558$, $F_{potency} = 0.2935$ and $P = 0.1841$, $F_{efficacy} = 2.273$, one-way ANOVA) and to the *cnr2*WT and the *cnr2*KO mice ($P = 0.6386$, $F_{potency} = 0.4837$ and $P = 0.1638$, $F_{efficacy} = 2.483$, one-way ANOVA). Thus, differences observed in the i.paw and the i.t. morphine analgesic effectiveness are apparently not caused by a decrease in the functional activity of spinal MOP within the different genotypes, as the ability of morphine to activate G protein is not modified. Along with previous results, these data provide direct evidence of apparently normal functional activity of spinal MOP in wild-type and knockout mice.

DISCUSSION

In the present study, we demonstrated that the inactivation of either CB_1 or CB_2 receptors in mice impairs the analgesic effects of i.paw and i.t. morphine when assessed with the formalin test. By contrast, the analgesic effectiveness of s.c. morphine was preserved in these transgenic mice, both in the formalin test and in the hot water immersion tail-flick test. We found that the loss of analgesic effectiveness of morphine was neither the consequence of impaired expression and binding properties of MOP, nor of its G protein coupling efficiency. Although we have not identified the exact mechanisms by which cannabinoid receptors influence morphine-induced analgesia, our findings further support the existence of a functional interaction between the cannabinoid and opioid systems, at least in the periphery and in the spinal cord.

It is now well recognized that the endocannabinoid and opioid systems share similar distributions in several brain areas as well as in the spinal cord and in the peripheral sites of pain processing (Di Marzo, 2008; Bodnar, 2012). Even if the molecular and cellular mechanisms involved in this process are not clearly established, cannabinoids and opioids are known to produce analgesic synergy in various animal models of pain (Welch, 2009; Parolaro et al., 2010). Indeed, previous studies using selective cannabinoid receptor antagonists have suggested that CB_1 receptors are involved in peripheral (da Fonseca Pacheco et al., 2008) and central morphine antinociception (Pacheco Dda et al., 2009) and that CB_2 receptors are partially involved in these effects (da Fonseca Pacheco et al., 2008). By contrast, the antinociceptive effects of systemic morphine remained unaffected by CB_1 receptor ablation in response to both chemical (Miller et al., 2011) and thermal noxious stimuli (Ledent et al., 1999; Valverde et al., 2000; Miller et al., 2011). In fact, the roles of CB_1 receptors described by pharmacological studies performed in wild-type mice were often not confirmed by studies using *cnr1*KO mice (Miller et al., 2011; Raffa and Ward, 2012). Notably, most studies using pharmacological tools have employed the high-affinity CB_1 antagonist/inverse agonist AM251 to investigate potential interactions between MOP and CB_1 receptors (Trang et al., 2007; da Fonseca Pacheco et al., 2008; Haghparast et al., 2009; Pacheco Dda et al., 2009). However, AM251 was recently found to display direct antagonist properties with respect to MOP (Seely et al., 2012). Therefore, some of the reported effects of this antagonist on MOP functions may not be mediated by the CB_1 receptors but rather by a direct action on MOP (Seely et al., 2012), which might explain the discrepancies between pharmacological and genetic approaches (Miller et al., 2011).

To better characterize the roles of the CB_1 and CB_2 receptors in modulating the opioid system, we studied the impact of disrupting these receptors on morphine-induced analgesia in mice. While our experiments, performed in knockout animals, exclude potential confounding effects of cannabinoid receptor antagonists, one could still argue that genetically modified mice may develop unidentified adaptations that could mask the role of cannabinoid receptors (Miller et al., 2011). However, it was shown that disruption of CB_1 receptors did not alter the mRNA levels of MOP in mouse dorsal root ganglia and spinal cord (Hojo et al., 2008). By contrast, *cnr1*KO mice were shown to have increased brain levels of substance P, enkephalin, and dynorphin (Zimmer et al., 1999). Regarding opioids, this observation might indicate a role for CB_1 in the tonic regulation of these peptides rather than a consequence of developmental adaptation. Although there is still no information regarding putative developmental changes in response to CB_2 receptor inactivation, there is no reason to believe that the loss of morphine analgesia observed in our study is the result of compensatory

modifications occurring in *cnr1*KO and *cnr2*KO mice. Indeed, in our experiments, the mice were found to behave normally, to be equally sensitive to i.d. formalin and to tail immersion in hot water, and to develop similar levels of formalin-induced edema and inflammation.

Aside from adaptation, direct receptor–receptor interaction and interaction between intracellular pathways are other putative mechanisms able to impede morphine-induced analgesia in *cnr1*KO and *cnr2*KO mice. Indeed, MOP and CB_1 receptors were shown to physically interact when co-expressed in the same cells (Rios et al., 2006). Physical interaction between the MOP and the CB_1 receptors was also evidenced by another group that used electrophysiological approaches to demonstrate the existence of a functional heterodimer (Hojo et al., 2008). *In vivo*, heterodimer formation requires that both receptors co-localize in the same neuron. Hence, it has been demonstrated that MOP and CB_1 receptors co-localize in dendritic spines in the caudate putamen, periaqueductal gray, dorsal horn of the spinal cord and presynaptic terminals (Hohmann et al., 1999; Rodriguez et al., 2001; Salio et al., 2001; Pickel et al., 2004; Vigano et al., 2005; Wilson-Poe et al., 2012). Another study has recently described functional interactions between forebrain MOP and CB_2 receptors and the impact of this interaction on agonist-mediated signaling (Paldyova et al., 2008). There is growing evidence that heterodimerization can generate receptors with novel pharmacological properties (Jordan and Devi, 1999; Bouvier, 2001; Devi, 2001). Indeed, the attenuation of CB_1 receptor-mediated signaling following MOP activation (Rios et al., 2006) or a decrease in the functions of MOP induced by the constitutive activity of CB_1 receptors (Canals and Milligan, 2008) have been shown. A recent study demonstrated that there is a decrease in DOP activity associated to its interaction with CB_1 receptors (Bushlin et al., 2012), therefore suggesting that cannabinoid receptors may have important impacts on opioid receptor functions. In the present study, we have demonstrated that there were no significant differences in the pattern of spinal MOP expression nor in its binding properties in wild-type mice compared to *cnr1*KO and *cnr2*KO mice. Moreover, we found that both the efficacy and the potency of spinal MOP's G protein coupling remained unaffected by CB_1 or CB_2 inactivation. It is therefore unlikely that the loss of morphine analgesia in *cnr1*KO and *cnr2*KO mice is the consequence of spinal MOP malfunction or downregulation due to the absence of MOP's heterodimerization with either CB_1 or CB_2 receptors. Admittedly however, our experimental design cannot exclude the possibility that cannabinoid receptors interfered with intracellular pathways of MOP, downstream of G proteins.

One could argue that the loss of morphine analgesia in *cnr1*KO and *cnr2*KO mice can be the consequence of a direct effect of morphine on cannabinoid receptors. However, the analgesic effects of morphine were often shown to be completely abolished in MOP KO animals demonstrating that the effects of morphine is mainly mediated by this receptor, at least *in vivo* (Matthes et al., 1996; Sora et al., 2001; Mizoguchi et al., 2003). Another mechanism that may explain our observations is the possibility that transgenic mice have a disrupted basal endocannabinoid tone that impairs the ability of i.paw and i.t. morphine to produce antinociception. Endocannabinoids were in fact shown to be involved in the regulation of antinociception following i.paw (da Fonseca Pacheco et al., 2008) and intracerebroventricular (i.c.v.) (Pacheco Dda et al., 2009) injections of morphine. Indeed, although brain levels of endocannabinoids remained unchanged after the acute administration of morphine, chronic treatment with morphine produced a widespread decrease in brain 2-arachidonoylglycerol (2-AG) without significantly changing anandamide levels (Vigano et al., 2003). In support of a role of endocannabinoids in i.paw and i.t. morphine-induced analgesia, we observed different consequences of CB_1 and CB_2 receptors invalidation in the antinociceptive effects of morphine on the two phases of the formalin test. While we found that morphine analgesia was attenuated in both phases of the formalin test in the *cnr1*KO mice, the *cnr2*KO mice only showed different effects of morphine-induced analgesia in the inflammatory phase. A possible interpretation of these results is that following i.paw and i.t. morphine administration, anandamide (high-affinity CB_1 agonist/low-affinity CB_2 agonist) may be rapidly released to primarily act at CB_1 receptors, thus participating in the attenuation of the early stages of nociception of the formalin test. In *cnr1*KO mice, the analgesic effect of anandamide on the first phase of the formalin test would be absent while it would remain unchanged in *cnr2*KO mice (due to the presence of CB_1). By contrast, the release of the non-selective endogenous 2-AG may produce a more sustained modulatory effect on inflammatory pain *via* both CB_1 and CB_2 receptors.

At first glance, it might appear puzzling that s.c. morphine-induced analgesia remained unaffected in both the formalin test and the tail-flick test. Indeed, previous studies have demonstrated that morphine analgesic efficacy requires activity at both spinal and supraspinal sites (Siuciak and Advokat, 1989; Miaskowski et al., 1993; Rossi et al., 1993; Kolesnikov et al., 1996). Analgesic synergy between MOP and CB_1 receptor agonists, ibuprofen, and paracetamol (the latter modulate cannabinoid synthesis) was also shown to play an important role in morphine analgesia (Fletcher et al., 1997; Kolesnikov et al., 2003; Tham et al., 2005; Kolesnikov and Soritsa, 2008; Mitchell et al., 2010). Based on these studies, it would have been logical to observe an attenuation of the analgesic efficacy of systemic morphine due to a lack/reduction of a spinal contribution. However, we found that the analgesic potency of s.c. morphine was preserved in both the formalin and the hot water immersion tail-flick tests. Our observations rather suggest that systemic morphine principally act *via* a neuronal network independent of cannabinoid receptors which therefore remain unaffected

in *cnr1*KO and *cnr2*KO mice. Consequently, the participation of spinal MOP in the analgesic effects of systemic morphine would be minimal since i.t. morphine analgesia is impaired in the same genotypes. In support to this hypothesis, a series of studies have shown that systemic morphine produces antinociception principally *via* the activation of descending inhibitory projections releasing serotonin in the dorsal horn of the spinal cord (Kuraishi et al., 1983; Giordano and Barr, 1988; Dogrul and Seyrek, 2006; Dogrul et al., 2009). The latter studies in fact revealed that blockade of spinal serotonin receptors or pharmacological depletion of serotonin in the spinal cord attenuates the analgesic effects of systemic and intracranial morphine (Kuraishi et al., 1983; Giordano and Barr, 1988; Dogrul and Seyrek, 2006; Dogrul et al., 2009) as well as other opioid receptor agonists such as tramadol (Yanarates et al., 2010).

CONCLUSION

We have demonstrated that peripheral and spinal antinociceptive effects of morphine were decreased in the inflammatory phase of the formalin test in *cnr1*KO and *cnr2*KO mice, whereas its systemic effects were preserved. These observations further support the existence of interactions between the cannabinoid and opioid systems. The loss of peripheral and spinal morphine analgesia is apparently caused neither by a decrease in MOP spinal expression nor by altered binding properties or G protein coupling of this receptor in *cnr1*KO and *cnr2*KO mice. The mechanisms underlying the loss of morphine analgesia are not clear but could include the release of endogenous cannabinoids in structures along the pain pathway or a disrupted endocannabinoid tone.

CONFLICT OF INTEREST

The authors report no conflict of interest.

Acknowledgments—The authors are thankful to Hélène Beaudry, Kristina Rochon, Sophie Charron, and Florence Dotigny for providing technical assistance with immunofluorescence experiments, saturation binding assays, and transgenic animals. We would also like to thank Dr. Michael Bruchas for advice with the GTPγS assay. This work was supported by a grant from the Fonds de Recherche Québec – Santé (FRQS)-funded Quebec Pain Research Network (QPRN) to PB-LG-JFB, by grants from the Natural Sciences and Engineering Research Council of Canada (NSERC) to JFB and LG and from the Canadian Institutes of Health Research (CIHR) to LG. JD is supported by a Vanier Canada Graduate Scholarships (#204685) from the CIHR. LG and JFB are recipients of FRQS Junior 2 salary supports. We would also like to thank Dr. Beat Lutz for providing the cnr1KO mice.

REFERENCES

Agarwal N, Pacher P, Tegeder I, Amaya F, Constantin CE, Brenner GJ, Rubino T, Michalski CW, Marsicano G, Monory K, Mackie K, Marian C, Batkai S, Parolaro D, Fischer MJ, Reeh P, Kunos G, Kress M, Lutz B, Woolf CJ, Kuner R (2007) Cannabinoids mediate analgesia largely via peripheral type 1 cannabinoid receptors in nociceptors. Nat Neurosci 10:870–879.

Beltramo M, Bernardini N, Bertorelli R, Campanella M, Nicolussi E, Fredduzzi S, Reggiani A (2006) CB2 receptor-mediated antihyperalgesia: possible direct involvement of neural mechanisms. Eur J Neurosci 23:1530–1538.

Bidaut-Russell M, Devane WA, Howlett AC (1990) Cannabinoid receptors and modulation of cyclic AMP accumulation in the rat brain. J Neurochem 55:21–26.

Bodnar RJ (2012) Endogenous opiates and behavior: 2011. Peptides 38:463–522.

Bouvier M (2001) Oligomerization of G-protein-coupled transmitter receptors. Nat Rev Neurosci 2:274–286.

Bushlin I, Gupta A, Stockton Jr SD, Miller LK, Devi LA (2012) Dimerization with cannabinoid receptors allosterically modulates delta opioid receptor activity during neuropathic pain. PloS One 7:e49789.

Canals M, Milligan G (2008) Constitutive activity of the cannabinoid CB1 receptor regulates the function of co-expressed Mu opioid receptors. J Biol Chem 283:11424–11434.

Chen Y, Mestek A, Liu J, Yu L (1993) Molecular cloning of a rat kappa opioid receptor reveals sequence similarities to the mu and delta opioid receptors. Biochem J 295(Pt 3):625–628.

Childers SR, Fleming L, Konkoy C, Marckel D, Pacheco M, Sexton T, Ward S (1992) Opioid and cannabinoid receptor inhibition of adenylyl cyclase in brain. Ann NY Acad Sci 654:33–51.

Cichewicz DL (2004) Synergistic interactions between cannabinoid and opioid analgesics. Life Sci 74:1317–1324.

Coderre TJ, Fundytus ME, McKenna JE, Dalal S, Melzack R (1993) The formalin test: a validation of the weighted-scores method of behavioural pain rating. Pain 54:43–50.

da Fonseca Pacheco D, Klein A, de Castro Perez A, da Fonseca Pacheco CM, de Francischi JN, Duarte ID (2008) The mu-opioid receptor agonist morphine, but not agonists at delta- or kappa-opioid receptors, induces peripheral antinociception mediated by cannabinoid receptors. Br J Pharmacol 154:1143–1149.

Devi LA (2001) Heterodimerization of G-protein-coupled receptors: pharmacology, signaling and trafficking. Trends Pharmacol Sci 22:532–537.

Di Marzo V (2008) Targeting the endocannabinoid system: to enhance or reduce? Nat Rev Drug Discov 7:438–455.

Dogrul A, Ossipov MH, Porreca F (2009) Differential mediation of descending pain facilitation and inhibition by spinal 5HT-3 and 5HT-7 receptors. Brain Res 1280:52–59.

Dogrul A, Seyrek M (2006) Systemic morphine produce antinociception mediated by spinal 5-HT7, but not 5-HT1A and 5-HT2 receptors in the spinal cord. Br J Pharmacol 149: 498–505.

Dubuisson D, Dennis SG (1977) The formalin test: a quantitative study of the analgesic effects of morphine, meperidine, and brain stem stimulation in rats and cats. Pain 4:161–174.

Evans CJ, Keith Jr DE, Morrison H, Magendzo K, Edwards RH (1992) Cloning of a delta opioid receptor by functional expression. Science (New York, NY) 258:1952–1955.

Fairbanks CA (2003) Spinal delivery of analgesics in experimental models of pain and analgesia. Adv Drug Deliv Rev 55:1007–1041.

Fletcher D, Benoist JM, Gautron M, Guilbaud G (1997) Isobolographic analysis of interactions between intravenous morphine, propacetamol, and diclofenac in carrageenin-injected rats. Anesthesiology 87:317–326.

Galiegue S, Mary S, Marchand J, Dussossoy D, Carriere D, Carayon P, Bouaboula M, Shire D, Le Fur G, Casellas P (1995) Expression of central and peripheral cannabinoid receptors in human immune tissues and leukocyte subpopulations. Eur J Biochem/FEBS 232:54–61.

Gendron L, Pintar JE, Chavkin C (2007) Essential role of mu opioid receptor in the regulation of delta opioid receptor-mediated antihyperalgesia. Neuroscience 150:807–817.

Giordano J, Barr GA (1988) Effects of neonatal spinal cord serotonin depletion on opiate-induced analgesia in tests of thermal and mechanical pain. Brain Res 469:121–127.

Guindon J, Desroches J, Beaulieu P (2007) The antinociceptive effects of intraplantar injections of 2-arachidonoyl glycerol

are mediated by cannabinoid CB2 receptors. Br J Pharmacol 150:693–701.
Haghparast A, Azizi P, Hassanpour-Ezatti M, Khorrami H, Naderi N (2009) Sub-chronic administration of AM251, CB1 receptor antagonist, within the nucleus accumbens induced sensitization to morphine in the rat. Neuroscience Lett 467:43–47.
Hohmann AG (2002) Spinal and peripheral mechanisms of cannabinoid antinociception: behavioral, neurophysiological and neuroanatomical perspectives. Chem Phys Lipids 121:173–190.
Hohmann AG, Briley EM, Herkenham M (1999) Pre- and postsynaptic distribution of cannabinoid and mu opioid receptors in rat spinal cord. Brain Res 822:17–25.
Hojo M, Sudo Y, Ando Y, Minami K, Takada M, Matsubara T, Kanaide M, Taniyama K, Sumikawa K, Uezono Y (2008) mu-Opioid receptor forms a functional heterodimer with cannabinoid CB1 receptor: electrophysiological and FRET assay analysis. J Pharmacol Sci 108:308–319.
Howlett AC (1995) Pharmacology of cannabinoid receptors. Annu Rev Pharmacol Toxicol 35:607–634.
Jhaveri MD, Sagar DR, Elmes SJ, Kendall DA, Chapman V (2007) Cannabinoid CB2 receptor-mediated anti-nociception in models of acute and chronic pain. Molecular neurobiology 36:26–35.
Jordan BA, Devi LA (1999) G-protein-coupled receptor heterodimerization modulates receptor function. Nature 399:697–700.
Kieffer BL, Befort K, Gaveriaux-Ruff C, Hirth CG (1992) The delta-opioid receptor: isolation of a cDNA by expression cloning and pharmacological characterization. Proc Natl Acad Sci U S A 89:12048–12052.
Kolesnikov Y, Soritsa D (2008) Analgesic synergy between topical opioids and topical non-steroidal anti-inflammatory drugs in the mouse model of thermal pain. Eur J Pharmacol 579:126–133.
Kolesnikov YA, Jain S, Wilson R, Pasternak GW (1996) Peripheral morphine analgesia: synergy with central sites and a target of morphine tolerance. J Pharmacol Exp Ther 279:502–506.
Kolesnikov YA, Wilson RS, Pasternak GW (2003) The synergistic analgesic interactions between hydrocodone and ibuprofen. Anesth Analg 97:1721–1723.
Kuraishi Y, Harada Y, Aratani S, Satoh M, Takagi H (1983) Separate involvement of the spinal noradrenergic and serotonergic systems in morphine analgesia: the differences in mechanical and thermal algesic tests. Brain Res 273:245–252.
Ledent C, Valverde O, Cossu G, Petitet F, Aubert JF, Beslot F, Bohme GA, Imperato A, Pedrazzini T, Roques BP, Vassart G, Fratta W, Parmentier M (1999) Unresponsiveness to cannabinoids and reduced addictive effects of opiates in CB1 receptor knockout mice. Science (New York, NY) 283:401–404.
Lever IJ, Rice AS (2007) Cannabinoids and pain. Handb Exp Pharmacol 177:265–306.
Lowry OH, Rosebrough NJ, Farr AL, Randall RJ (1951) Protein measurement with the Folin phenol reagent. J Biol Chem 193:265–275.
Maldonado R, Valverde O (2003) Participation of the opioid system in cannabinoid-induced antinociception and emotional-like responses. Eur Neuropsychopharmacol 13:401–410.
Manzanares J, Corchero J, Romero J, Fernandez-Ruiz JJ, Ramos JA, Fuentes JA (1999) Pharmacological and biochemical interactions between opioids and cannabinoids. Trends Pharmacol Sci 20:287–294.
Massi P, Vaccani A, Romorini S, Parolaro D (2001) Comparative characterization in the rat of the interaction between cannabinoids and opiates for their immunosuppressive and analgesic effects. J Neuroimmunol 117:116–124.
Matsuda LA, Lolait SJ, Brownstein MJ, Young AC, Bonner TI (1990) Structure of a cannabinoid receptor and functional expression of the cloned cDNA. Nature 346:561–564.
Matthes HW, Maldonado R, Simonin F, Valverde O, Slowe S, Kitchen I, Befort K, Dierich A, Le Meur M, Dolle P, Tzavara E, Hanoune J, Roques BP, Kieffer BL (1996) Loss of morphine-induced analgesia, reward effect and withdrawal symptoms in mice lacking the mu-opioid-receptor gene. Nature 383:819–823.
Miaskowski C, Taiwo YO, Levine JD (1993) Antinociception produced by receptor selective opioids. Modulation of supraspinal antinociceptive effects by spinal opioids. Brain Res 608:87–94.
Miller LL, Picker MJ, Schmidt KT, Dykstra LA (2011) Effects of morphine on pain-elicited and pain-suppressed behavior in CB1 knockout and wildtype mice. Psychopharmacology 215: 455–465.
Mitchell D, Gelgor L, Weber J, Kamerman PR (2010) Antihypernociceptive synergy between ibuprofen, paracetamol and codeine in rats. Eur J Pharmacol 642:86–92.
Mizoguchi H, Wu HE, Narita M, Sora I, Hall SF, Uhl GR, Loh HH, Nagase H, Tseng LF (2003) Lack of mu-opioid receptor-mediated G-protein activation in the spinal cord of mice lacking Exon 1 or Exons 2 and 3 of the MOR-1 gene. J Pharmacol Sci 93:423–429.
Munro S, Thomas KL, Abu-Shaar M (1993) Molecular characterization of a peripheral receptor for cannabinoids. Nature 365:61–65.
Pacheco Dda F, Klein A, Perez AC, Pacheco CM, de Francischi JN, Reis GM, Duarte ID (2009) Central antinociception induced by mu-opioid receptor agonist morphine, but not delta- or kappa-, is mediated by cannabinoid CB1 receptor. Br J Pharmacol 158:225–231.
Paldy E, Bereczki E, Santha M, Wenger T, Borsodi A, Zimmer A, Benyhe S (2008) CB(2) cannabinoid receptor antagonist SR144528 decreases mu-opioid receptor expression and activation in mouse brainstem: role of CB(2) receptor in pain. Neurochem Int 53:309–316.
Paldyova E, Bereczki E, Santha M, Wenger T, Borsodi A, Benyhe S (2008) Noladin ether, a putative endocannabinoid, inhibits mu-opioid receptor activation via CB2 cannabinoid receptors. Neurochem Int 52:321–328.
Parolaro D, Rubino T, Vigano D, Massi P, Guidali C, Realini N (2010) Cellular mechanisms underlying the interaction between cannabinoid and opioid system. Curr Drug Targets 11:393–405.
Petricevic M, Wanek K, Denko CW (1978) A new mechanical method for measuring rat paw edema. Annu Rev Pharmacol Toxicol 16:153–158.
Pickel VM, Chan J, Kash TL, Rodriguez JJ, MacKie K (2004) Compartment-specific localization of cannabinoid 1 (CB1) and mu-opioid receptors in rat nucleus accumbens. Neuroscience 127:101–112.
Pol O, Puig MM (2004) Expression of opioid receptors during peripheral inflammation. Curr Top Med Chem 4:51–61.
Raffa RB, Ward SJ (2012) CB(1)-independent mechanisms of Delta(9)-THCV, AM251 and SR141716 (rimonabant). J Clin Pharm Ther 37:260–265.
Rios C, Gomes I, Devi LA (2006) mu opioid and CB1 cannabinoid receptor interactions: reciprocal inhibition of receptor signaling and neuritogenesis. Br J Pharmacol 148:387–395.
Rodriguez JJ, Mackie K, Pickel VM (2001) Ultrastructural localization of the CB1 cannabinoid receptor in mu-opioid receptor patches of the rat Caudate putamen nucleus. J Neurosci 21:823–833.
Rossi GC, Pasternak GW, Bodnar RJ (1993) Synergistic brainstem interactions for morphine analgesia. Brain Res 624:171–180.
Salio C, Fischer J, Franzoni MF, Mackie K, Kaneko T, Conrath M (2001) CB1-cannabinoid and mu-opioid receptor co-localization on postsynaptic target in the rat dorsal horn. Neuroreport 12:3689–3692.
Schatz AR, Lee M, Condie RB, Pulaski JT, Kaminski NE (1997) Cannabinoid receptors CB1 and CB2: a characterization of expression and adenylate cyclase modulation within the immune system. Toxicol Appl Pharmacol 142:278–287.
Seely KA, Brents LK, Franks LN, Rajasekaran M, Zimmerman SM, Fantegrossi WE, Prather PL (2012) AM-251 and rimonabant act as direct antagonists at mu-opioid receptors: implications for opioid/cannabinoid interaction studies. Neuropharmacology 63:905–915.
Siuciak JA, Advokat C (1989) The synergistic effect of concurrent spinal and supraspinal opiate agonisms is reduced by both nociceptive and morphine pretreatment. Pharmacol Biochem Behav 34:265–273.

Sora I, Elmer G, Funada M, Pieper J, Li XF, Hall FS, Uhl GR (2001) Mu opiate receptor gene dose effects on different morphine actions: evidence for differential in vivo mu receptor reserve. Neuropsychopharmacology 25:41–54.

Tham SM, Angus JA, Tudor EM, Wright CE (2005) Synergistic and additive interactions of the cannabinoid agonist CP55,940 with mu opioid receptor and alpha2-adrenoceptor agonists in acute pain models in mice. Br J Pharmacol 144:875–884.

Tjolsen A, Berge OG, Hunskaar S, Rosland JH, Hole K (1992) The formalin test: an evaluation of the method. Pain 51:5–17.

Trang T, Sutak M, Jhamandas K (2007) Involvement of cannabinoid (CB1)-receptors in the development and maintenance of opioid tolerance. Neuroscience 146:1275–1288.

Valverde O, Ledent C, Beslot F, Parmentier M, Roques BP (2000) Reduction of stress-induced analgesia but not of exogenous opioid effects in mice lacking CB1 receptors. Eur J Neurosci 12:533–539.

Van Sickle MD, Duncan M, Kingsley PJ, Mouihate A, Urbani P, Mackie K, Stella N, Makriyannis A, Piomelli D, Davison JS, Marnett LJ, Di Marzo V, Pittman QJ, Patel KD, Sharkey KA (2005) Identification and functional characterization of brainstem cannabinoid CB2 receptors. Science (New York, NY) 310:329–332.

Vigano D, Grazia Cascio M, Rubino T, Fezza F, Vaccani A, Di Marzo V, Parolaro D (2003) Chronic morphine modulates the contents of the endocannabinoid, 2-arachidonoyl glycerol, in rat brain. Neuropsychopharmacology 28:1160–1167.

Vigano D, Rubino T, Parolaro D (2005) Molecular and cellular basis of cannabinoid and opioid interactions. Pharmacol Biochem Behav 81:360–368.

Walczak JS, Pichette V, Leblond F, Desbiens K, Beaulieu P (2005) Behavioral, pharmacological and molecular characterization of the saphenous nerve partial ligation: a new model of neuropathic pain. Neuroscience 132:1093–1102.

Walczak JS, Pichette V, Leblond F, Desbiens K, Beaulieu P (2006) Characterization of chronic constriction of the saphenous nerve, a model of neuropathic pain in mice showing rapid molecular and electrophysiological changes. J Neurosci Res 83:1310–1322.

Welch SP (2009) Interaction of the cannabinoid and opioid systems in the modulation of nociception. Int Rev Psychiatry (Abingdon, England) 21:143–151.

Wilson-Poe AR, Morgan MM, Aicher SA, Hegarty DM (2012) Distribution of CB1 cannabinoid receptors and their relationship with mu-opioid receptors in the rat periaqueductal gray. Neuroscience 213:191–200.

Yanarates O, Dogrul A, Yildirim V, Sahin A, Sizlan A, Seyrek M, Akgul O, Kozak O, Kurt E, Aypar U (2010) Spinal 5-HT7 receptors play an important role in the antinociceptive and antihyperalgesic effects of tramadol and its metabolite, O-desmethyltramadol, via activation of descending serotonergic pathways. Anesthesiology 112:696–710.

Yasuda K, Raynor K, Kong H, Breder CD, Takeda J, Reisine T, Bell GI (1993) Cloning and functional comparison of kappa and delta opioid receptors from mouse brain. Proc Natl Acad Sci U S A 90:6736–6740.

Zimmer A, Zimmer AM, Hohmann AG, Herkenham M, Bonner TI (1999) Increased mortality, hypoactivity, and hypoalgesia in cannabinoid CB1 receptor knockout mice. Proc Natl Acad Sci U S A 96:5780–5785.

(Accepted 13 December 2013)
(Available online 21 December 2013)